Zirconia Ceramics

Bedirhan Savas Yigit[1], Marwan Al-Akkad[1], Radek Mounajjed[1,2,*]

ABSTRACT
Zirconia ceramics have become popular among other dental ceramics thanks to their biological, mechanical, optical, and aesthetic properties. CAD/CAM (computer-aided design/ computer-aided manufacturing) technology improvement has played a vital role in the increased popularity of zirconia ceramics; easy computer manipulation significantly expanded the possibility of using different types of restorations. Zirconia ceramics have a broad spectrum of indications in prosthetic dentistry, from simple restorations to complex structures supported by dental implants. A good orientation in the classification, features, and manipulation of zirconia ceramics is the main key to success.

KEYWORDS
zirconia ceramics; adhesion; biokompatibility; production of zirconia

AUTHOR AFFILIATIONS
[1] Institute of Dentistry and Oral Sciences, Palacky University Olomouc, Olomouc, Czech Republic
[2] Private Clinician, DCM Clinic, Hradec Králové, Czech Republic
* Corresponding author: Institute of Dentistry and Oral Sciences, Palacky University Olomouc, Olomouc, Czech Republic; e-mail: mounajjed@me.com

Received: 19 June 2024
Accepted: 25 August 2024
Published online: 22 October 2024

Acta Medica (Hradec Králové) 2024; 67(2): 39–45
https://doi.org/10.14712/18059694.2024.18

INTRODUCTION

Prosthetic dentistry is undergoing a paradigm shift from metal-ceramic restorations to all-ceramic restorations (1). In order to replace metal-ceramic restorations, all ceramic restorations have been developed. Zirconia has differentiated itself among all dental ceramics as a versatile and promising material due to its biological, mechanical, and optical properties. CAD/CAM (computer-aided design / computer-aided manufacturing) technology has played a significant role in producing zirconia restorations (1, 2).

The name of the metal, Zirconium, originates from the Arabic and Persian origin, "Zargon", meaning "golden in color" (3, 4). Zirconia, the metal oxide ZrO_2, was first discovered in 1789 by German chemist Martin Heinrich Klaproth. In 1824, Swedish chemist Jöns Jakob Berzelius managed to isolate it for the first time (2–6). In 1975, Gravie et al. proposed a model to rationalize the desirable mechanical properties of zirconia, which has been called "ceramic steel" (7).

PHASES OF ZIRCONIA

Zirconia has a feature known as polymorphism, characterized by the atoms' geometric arrangement in different ways and different crystallographic structures. Zirconium oxide crystals are organized in crystalline structures, which can be divided into three crystallographic phases. The cubic (C) is in the form of a straight prism with square sides, the tetragonal (T) is in the form of a straight prism with rectangular sides, and the monoclinic (M) is in the form of a deformed prism with parallel sides (2, 5, 8).

Pure zirconia is in the monoclinic phase, which is stable at room temperature up to 1170 °C. Between 1170 °C and 2370 °C, tetragonal zirconia is formed, while cubic zirconia occurs above the temperature of 2370 °C until the melting point of 2716 °C (9, 10). Moreover, there are noticeable alterations in volume, which are related to this phase transformation. A significant volume increase of about 4.5% occurs along with the transformation from the tetragonal phase to the monoclinic phase during cooling, which creates a surface compressive stress within the material; thereby, flexural strength is increased (11). Moreover, phase change affects the integrity of the material. As a result, aging becomes more likely. (11, 12, 13).

STABILIZED ZIRCONIA

Stabilized zirconia is a combination of zirconia polymorphs obtained at room temperature by adding stabilizers (4). Passerini et al. (14) and Ruff et al. (15) found that the tetragonal and cubic phase could be stabilized at room temperature thanks to alloying zirconia with metal oxides such as CaO, MgO, Y_2O_3, CeO_2, Er_2O_3, Eu_2O_3, Gd_2O_3, Sc_2O_3, La_2O_3 and Yb_2O_3 (16). Amongst them, yttrium oxide (Y_2O_3) is the primary stabilizer used in general medicine and dentistry. The stabilization principle is based on replacing Zr^{4+} cations with Y^{3+} cations in the ZrO_2 crystal structure. Zr^{4+} is a tetravalent ion, while Y^{3+} is a trivalent ion. Replacing a tetravalent ion with a trivalent ion will cause one oxygen anion to remain free in the crystal structure. This free oxygen anion is called an oxygen vacancy, and it subsequently prevents the phase transformation (8, 17).

The amount of yttrium oxide has an influence on stabilization (17, 18). When the amount of yttrium oxide is over 8 mol%, the cubic phase becomes stable at room temperature, and it is called cubic stabilized zirconia (CSZ). When yttrium oxide is 3 to 8 mol%, both cubic and tetragonal phases are mixed at room temperature; it is called partially stabilized zirconia (PSZ). When the yttrium oxide is about 3 mol%, tetragonal phases are almost 100% at room temperatures. In this case, it is called tetragonal zirconia polycrystal (TZP) (18).

BIOCOMPATIBILITY

Zirconia's biocompatibility has been thoroughly assessed, and studies have proven its biocompatibility (12, 19, 20). No study found a difference or identified any modifications in the biological health of the soft and hard tissues around the zirconia-based restorations (13, 21–25).

PHASE TRANSFORMATION TOUGHENING (PTT)

The adsorbed energy can break some of the atomic bonds in a polycrystalline structure under the influence of mechanical, thermal, or combined stresses, leading to tetragonal crystals changing into a more stable monoclinic phase (metastability). Phase Transformation Toughening is the term used to describe this spontaneous and irreversible

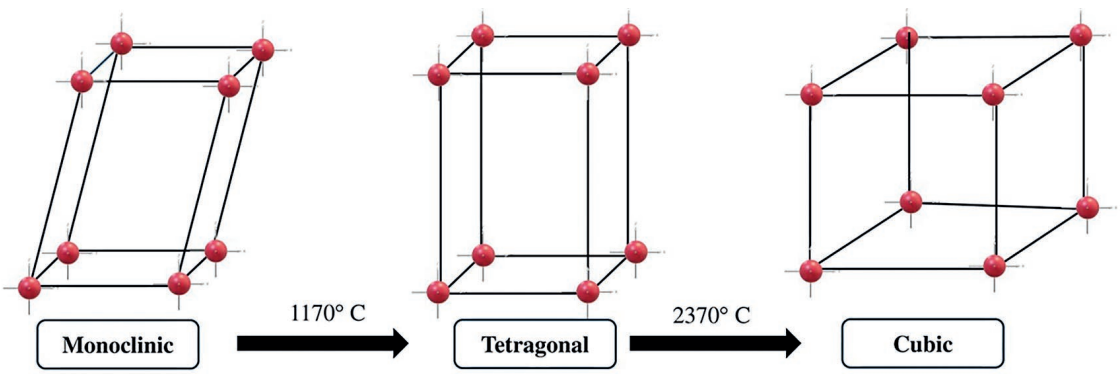

Fig. 1 Phases of zirconia.

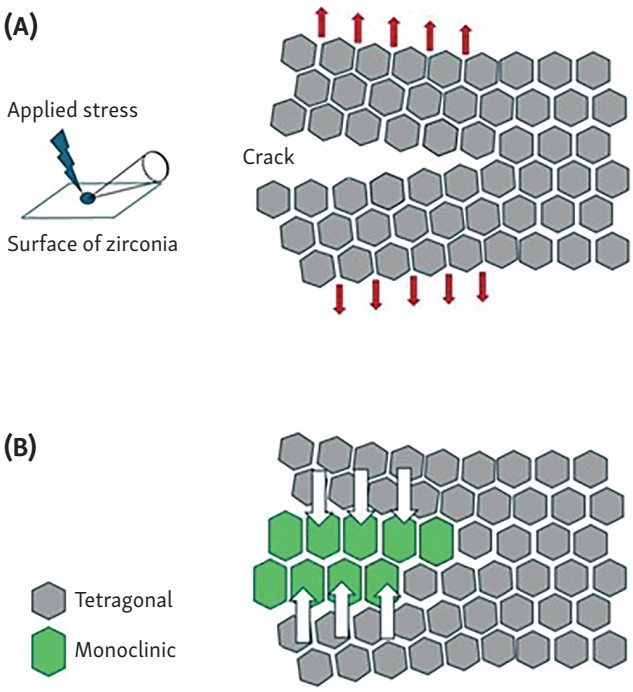

Fig. 2 Crack propagation and phase transformation toughening.

change. A crack can occur on the surface of a material if there is enough force. At that moment, the forces from the initial impulse act perpendicular to the crack surface, and the crack is spread until the forces causing crack expansion are no longer sufficient. In metastable tetragonal zirconia, these forces lead to local destabilization of the tetragonal phase, which results in tetragonal to monoclinic phase transformation. This creates a zone with a mixture of tetragonal and monoclinic phases. This phase transformation is related to volume expansion, which causes the crack to tighten and close (13, 17, 26).

From a technological point of view, PTT has been promoted as a significant improvement since it enables zirconia's self-repairability within the material (13, 26, 27).

LOW-TEMPERATURE DEGRADATION (LTD)

Low-temperature degradation (aging) is characterized by spontaneous irreversible transformation change from tetragonal to monoclinic phase, which occurs along the time at room temperature. LTD is a multifactorial phenomenon influenced by several variables, such as temperature, crystal dimension, surface defects, percentage and distribution of stabilizing oxide, wetness, and mechanical stress. Explicitly, the last two factors are the common causes of zirconia aging. LTD is known to cause worsening of zirconia's mechanical properties, contributing to the onset of microcracks and toughness reduction (13, 26, 28–30).

THE MANUFACTURING PROCEDURE FOR ZIRCONIA

Zirconia restorations can be fabricated by CAD/CAM milling based on two different production methods: soft machining of pre-sintered or hard machining of fully sintered zirconia or additvive manufacturing (13, 32).

Soft machining is the most used method based on the milling of pre-sintered zirconia blanks (Green state) made by cold isostatic pressing, a mixture of zirconia powder, stabilizing oxides, and a binding agent (13). With this method, zirconia is very homogenous, and the milling procedure is easier. Production time, machinery wear, and the number of surface defects are decreased. However, 20–30% of oversizing is required for this milling process due to sintering shrinkage (11, 13, 31).

Hard machining is done by milling fully sintered zirconia produced by hot isostatic pressing at 1400–1500 °C (2, 4). This method eradicates the shrinkage problem after milling since there is no need for oversizing (11, 31). Due to the high hardness and low machinability of fully sintered zirconia, a longer milling time is required. Moreover, zirconia may undergo monolithic phase change after the hard machining process because of mechanical stress, working burs friction, and overheating, which can affect the mechanical properties of zirconia (11–13, 31).

Additive manufacturing is a technique that describes successive adding and joining materials, whether in powder or liquid form, layer by layer of fabricate prosthesis using a 3D printer. This approach comes in many different forms such as material extrusion, powder bed fusion, plaster-based 3D printing, laminated item production, stereolithography, and polyjet 3D printing. The advantages of this technology are extensive, offering almost limitless design possibilities, the ability to create complex structures in a single production cycle, user-friendly operation, and the flexibility to customize colors and materials for

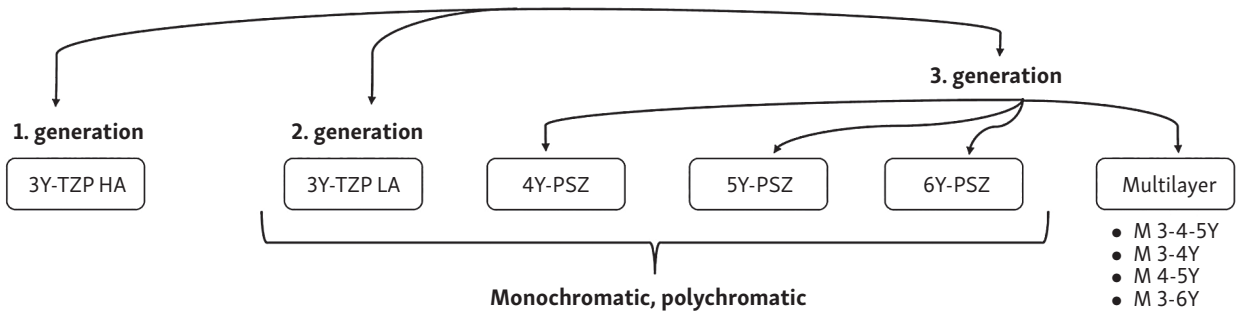

Fig. 3 Zirconia classification.

different sections of the print. However there are challanges related to this method such as the high costs of the required machines and software, limitations on the types of materials that can be used, and high sensitivity to inconsistencies in the input data (32–35).

ZIRCONIA CLASSIFICATION

1. First generation of zirconia ceramics 3 mol% yttria-stabilized tetragonal zirconia polycrystalline with high alumina content (3Y-TZP HA)

The first zirconia ceramics used for dental applications was 3Y-TZP HA, conventional zirconia, which contains 0.25–0.5 wt% alumina and 3 mol% Y_2O_3 (1) and 100% tetragonal crystals. These types of ceramics began to be used for their high toughness and flexural strength, which is bigger than 1GPa (2, 5, 37). Their indications are limited due to a lack of aesthetics (10). They display considerable opacity due to their natural birefringence of noncubic zirconia, which leads to light scattering from grain boundaries and pores (10). As a result, they are mainly indicated as a framework for porcelain-veneered crowns and fixed dental prostheses in the posterior region (10, 36, 37).

2. Second generation of zirconia ceramics 3 mol% yttria-stabilized tetragonal zirconia polycrystalline with less alumina content (3Y-TZP LA)

The composition of these types of zirconia has been changed to enhance translucency. Alumina content was decreased to less than 0.05 wt%, and the sintering temperature was increased (10, 31, 37). In this way, porosity was eliminated, and alumina grains were reduced, and within the zirconia, the latter were repositioned, which occurs on grain boundaries of zirconia (31). Therefore, high light transmittance and high strength were achieved together (31). On the contrary, this type of zirconia ceramic contains metastable tetragonal zirconia, which limits translucency (17). Due to esthetic reasons, they are not used in the anterior region. However, they are used for single crowns for posterior regions and long-span bridges (17, 38).

3. Third generation of zirconia ceramics (4Y-PSZ, 5Y-PSZ, 6Y-PSZ)

The desire for more translucent zirconia ceramic emerged because of the esthetic inadequacy of the second generation of zirconia ceramic compared to glass ceramics in terms of translucency (31, 33). This led to the development of the third generation of zirconia ceramic by increasing yttria content up to 4 mol%, 5 mol%, or 6 mol% (10, 18, 31, 37). This zirconia, when compared to the first and second generation, contains not only a tetragonal phase but also a cubic phase in the proportion of up to 50 % (31). This significantly enhanced translucency; on the contrary, strength and toughness were reduced since cubic zirconia is not capable of transformation toughening (10, 18, 39). However, the volume of cubic crystals is bigger than that of tetragonal ones, which indicates that light scattering is less intense at the grain boundaries and porosity, which makes zirconia more translucent (31). Because of high translucency and lack of toughness, their indications are limited to anterior crowns and veneers (18).

Although the translucency of zirconia ceramics has improved over the years, they are monochromatic. So as to produce restorations that mimic the natural tooth appearance, polychromatic and multi-layered zirconia ceramics were developed (40). In polychromatic zirconia, among the different layers, the same amount of yttria content and cubic phase is observed (40). The main difference is pigment composition, which makes the difference in shade, not in translucency (41). A different approach has been used to produce multi-layered zirconia, where the same material contains different compositions of yttria and microstructures. The incisal layer is more translucent because it has more yttria content. However, increased yttria concentration reduces mechanical properties. The cervical layer is not as translucent as the incisal layer due to a lower concentration of yttria, but due to this, the cervical layer has higher mechanical strength than the incisal region. Between those two layers, there is a transition layer, which is a mixture of various types of yttrium oxide (40–43). Thanks to the unique property of transmission of shade and translucency, they have a broad spectrum of indications, including anterior crowns and veneer, with high esthetic expectations (18, 40).

ADHESION TO ZIRCONIA AND CEMENT SELECTION

Zirconia lacks an amorphous glassy matrix; because of this, it cannot be pre-conditioned by using hydrofluoric acid etching (13, 44). In order to achieve good adhesion to zirconia ceramics, several methods were suggested (44, 45). However, the first step for adhesion is to create a contaminant-free surface (45). This is carried out by polishing with papers, sprays, milling cutters of silicon carbide ranging between 220 to 4000 grit, ultrasonic cleaning, or using different solutions such as water, alcohol, acetone, ethanol, and isopropanol with a usage time between 1 to 10 minutes (44, 45). Special cleaning agents are recommended to use in order to eliminate surface contamination in the oral cavity after try-in (46, 47). Two commercial brands

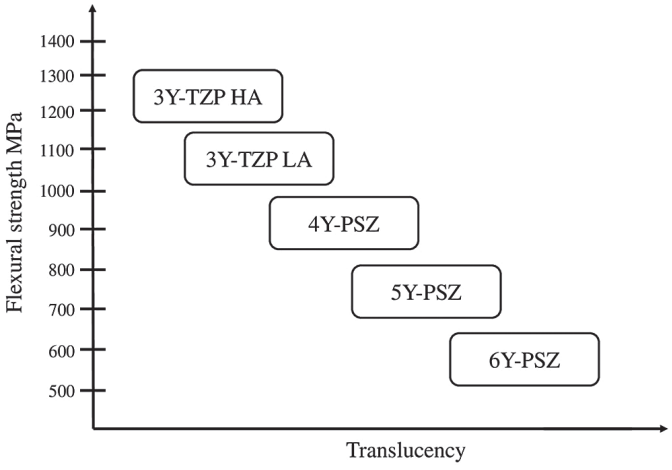

Fig. 4 Flexural strength and translucency.

are mostly used: Ivoclean and Katana cleaner. According to the manufacturer's scientific information, the effect of Ivoclean in removing saliva contaminants might be explained by the balance of chemical reactions, in which the direction of the solution balance relies on the concentration of the reaction partner. With a higher amount of one reactant, binding to that reactant is much more likely than to any other less common reactant. This material is composed of an alkaline suspension of zirconia particles; because of this, Ivoclean can be applied only extraorally before cementation. Phosphate contaminants from saliva on the surface of ceramic restoration will bind based on the size and concentration of these zirconia particles in Ivoclean, thus supporting the cleaning action on the zirconia surface (46, 47–49). Katana Cleaner is an acidic solution composed of 10-MDP (10-methacryloyloxydecyl dihydrogen phosphate) salts. Thanks to 10-MDP salts, Katana Cleaner can be used intraorally and extraorally. This chemical can neutralize fatty acids, adjust and buffer pH, and dissolve oils and other components that are not water-soluble. The hydrophobic part of the 10-MDP salt forms a bond with contaminants. In contrast, the hydrophilic part of the 10-MDP salt does not form bonds; thus, the contaminants can be removed by rinsing with water (46, 47, 50).

Sandblasting is a process that uses the energy discharged by the bounce of alumina particles that are generated by a high-speed source (45, 51). With this method, surface energy, roughness, wettability, and appearance of a hydroxyl group, which will create a bond between primer and cement, are increased (44). On the contrary, sandblasting can cause surface deformation, defects, and cracks; consequently, the mechanical properties of zirconia might be jeopardized (52). For this reason, it is essential to carry out this process based on adequate parameters regarding pressure, distance from the source, and particle size (44, 45, 53). These parameters vary in particle size from 30 to 110 μm, pressure from 0.5 to 4 bar, and distance from the source from 10 to 20 mm (44). However, 2 bar pressure and 50 μm particle size are recommended (54, 55–57).

Tribochemical silica coating is another approach to increase adhesion to zirconia (44, 45). It is a sandblasting process done by blasting alumina particles covered by silica onto the zirconia surface. (44, 45, 58). This process creates an uneven surface while fusing silica into a zirconia structure, allowing the application of silane as a coupling agent (44, 45, 59). This leads to the appearance of chemical chains of siloxane between cement and residual silica, increasing adhesion and improving the wettability and surface energy of zirconia (44). Tribochemical silica coating is done by two methods: the Rocatec system is based on the traditional sandblasting process followed by the use of silica-coated alumina particles (110 μm). Another system is the Cojet system, which uses alumina particles (50 μm) covered by silica, and the Cojet system can be performed at chair side (60). The pressure used with these systems ranges from 0.8 to 4 bar. However, crack propagation is observed when used at high pressure because a pressure of 1.8-2.8 bar is recommended to achieve a significant increase in adhesion (44, 51, 56).

Fusion sputtering, as described by Aboushelib (61), is a technique for creating a rough zirconia surface by spraying an air-water jet carrying microscopic zirconia particles (4–12 μm) on non-sintered zirconia (61, 62). After the sintering process, these microscopic non-sintered particles fuse to underlying zirconia. Therefore, surface area and surface roughness is increased (61–63). 3 bar, 7–12 μm particle size, 20 mm distance from a target, and 5-second application time were advised to obtain adequate adhesion to zirconia (62, 64).

Selective infiltration etching is another method to modify the zirconia surface (44, 45). Zirconia is covered by silica-based material, which diffuses within the zirconia structure at 960°C. Afterward, hydrofluoric acid is applied for about 10 minutes to dissolve the glass component. In this way, the zirconia surface becomes roughened (64, 65, 67, 68).

Lasers were also used to alter the surface of zirconia (44, 45, 63). The goal of laser application is to create a rough surface and increase wettability, which will allow micromechanical interconnection with the resin (69). Several types of lasers (Er: YAG, Nd: YAG, Yb: YAG, CO_2) have been used with different parameters of power, energy intensity, distance, and duration (70–72).

The hot acid etching method relies on a controlled corrosion process and the metallic character of zirconium (60). Acid selectively etches zirconia, and it creates micro-retention areas on the surface by removing less arranged atoms (63, 72). Various acidic solutions have been suggested, such as phosphoric acid, nitric acid, and hydrofluoric acid (68–70).

Functional monomers are those that show reactive side-chain groups whose purpose is to synthesize more complex compounds (75). They contain at least one polymerizable and functional group (76). However, 10-MDP (10-Methacryloyloxydecyl dihydrogen phosphate), 4-META (4- 4-methacryloyloxy ethyl trimellitate anhydride), 6-MHPA (6-methacryloyloxy ethyl phosphonoacetate), 3-TMSPMA (3-(Trimethoxysilyl) propyl methacrylate), MAC-10 (11-methacryloyloxy-1,1-undecane dicarboxylic acid) are used. 10-MDP is currently the most popular functional monomer since it provides long-term reliable adhesion (44, 45, 76). 10-MDP has two terminal groups. In one terminal, there is phosphoric acid, which gives a reaction with zirconia and creates a phosphate – oxygen – zirconium bond. At the other end of the molecule, there is a vinyl group that has a role in copolymerization with resin. Between these two groups, a carbon chain, which is responsible for viscosity, rigidity, hydrophobicity, and solubility, stands (44).

For zirconia cementation, conventional and adhesive resin cements are indicated (77, 78). Conventional cements are indicated for full coverage zirconia restorations, considering the simple and less demanding procedure (77). Adhesive cements are used to achieve better marginal seals and improve retention and fracture resistance (77).

CONCLUSION

Zirconia ceramics have shown significant technological development over the past ten years, which has led to a

wide range of applications. Zirconia ceramics are the ideal choice of material for demanding restorations and highly aesthetic constructions thanks to the unique features of zirconia ceramics, such as strength, resistance to wear, resistance to corrosion, and aesthetic features.

REFERENCES

1. Mao L, Kaizer MR, Zhao M, Guo B, Song YF, Zhang Y. Graded Ultra-Translucent Zirconia (5Y-PSZ) for Strength and Functionalities. J Dent Res. 2018 Oct; 97(11): 1222–8.
2. Kumar M, Razdan S, Sharma A. An Overview of Zirconia and its Application in Dentistry. Dent J Adv Stud. 2016 Apr; 04(01): 001–7.
3. Pilathadka S, Vahalová D, Vosáhlo T. The Zirconia: a new dental ceramic material. An overview. Prague Med Rep. 2007; 108(1): 5–12.
4. Vagkopoulou T, Koutayas SO, Koidis P, Strub JR. Zirconia in dentistry: Part 1. Discovering the nature of an upcoming bioceramic. Eur J Esthet Dent. 2009; 4(2): 130–51.
5. Saridag S, Tak O, Alniacik G. Basic properties and types of zirconia: An overview. WJS. 2013; 2(3): 40.
6. Alqutaibi AY, Ghulam O, Krsoum M, Binmahmoud S, Taher H, Elmalky W, et al. Revolution of Current Dental Zirconia: A Comprehensive Review. Molecules. 2022 Mar 4; 27(5): 1699.
7. Garvie RC, Hannink RH, Pascoe RT. Ceramic steel? Nature. 1975 Dec; 258(5537): 703–4.
8. Kelly J, Denry I. Stabilized zirconia as a structural ceramic: An overview. Dent Mater. 2008 Mar; 24(3): 289–98.
9. Ali S, Karthigeyan S, Deivanai M, Mani R. Zirconia Properties and Application – A Review. Pak Oral Dental J. 2014 Jan 1; 34: 178–83.
10. Zhang Y, Lawn BR. Novel Zirconia Materials in Dentistry. J Dent Res. 2018 Feb; 97(2): 140–7.
11. Denry I, Kelly J. State of the art of zirconia for dental applications. Dent Mater. 2008 Mar; 24(3): 299–307.
12. Piconi C, Maccauro G. Zirconia as a ceramic biomaterial. Biomaterials. 1999 Jan; 20(1): 1–25.
13. Zarone F, Di Mauro MI, Ausiello P, Ruggiero G, Sorrentino R. Current status on lithium disilicate and zirconia: a narrative review. BMC Oral Health. 2019 Dec; 19(1): 134.
14. Passerini L. Isomorphism among oxides of different tetravalentmetals: CeO2-ThO2; CeO2-ZrO2; CeO2-HfO2. Gazzet Chim Ital. 1939; 60: 762–776.
15. Ruff O, Ebert F. Refractory ceramics: I. The forms of zirkonium dioxide. Z Anorg Allg Chem. 1929; 180: 19–41.
16. Lughi V, Sergo V. Low temperature degradation -aging- of zirconia: A critical review of the relevant aspects in dentistry. Dent Mater. 2010 Aug; 26(8): 807–20.
17. Kovalský T, Voborná I, Míšová E, Rosa M, Polanská V, Hepová M, et al. Zirconia Ceramics: Properties and Classification. ČSPZL. 2022 Mar 1; 122(1): 11–6.
18. Ban S. Classification and Properties of Dental Zirconia as Implant Fixtures and Superstructures. Materials. 2021 Aug 27; 14(17): 4879.
19. Manicone PF, Rossi Iommetti P, Raffaelli L. An overview of zirconia ceramics: Basic properties and clinical applications. J Dent. 2007 Nov; 35(11): 819–26.
20. Lin H, Yin C, Mo A. Zirconia Based Dental Biomaterials: Structure, Mechanical Properties, Biocompatibility, Surface Modification, and Applications as Implant. Front Dent Med. 2021 Aug 3; 2: 689198.
21. Sharanraj V, Ramesha CM, Kavya K, Kumar V, Sadashiva M, Chandan BR, et al. Zirconia: as a biocompatible biomaterial used in dental implants. Adv Appl Ceram. 2021 Feb 17; 120(2): 63–8.
22. Gautam C, Joyner J, Gautam A, Rao J, Vajtai R. Zirconia based dental ceramics: structure, mechanical properties, biocompatibility and applications. Dalton Trans. 2016; 45(48): 19194–215.
23. Bona A, Pecho O, Alessandretti R. Zirconia as a Dental Biomaterial. Materials. 2015 Aug 4; 8(8): 4978–91.
24. Lohmann CH, Dean DD, Köster G, Casasola D, Buchhorn GH, Fink U, et al. Ceramic and PMMA particles differentially affect osteoblast phenotype. Biomaterials. 2002 Apr; 23(8): 1855–63.
25. Raigrodski AJ, Hillstead MB, Meng GK, Chung KH. Survival and complications of zirconia-based fixed dental prostheses: A systematic review. J Prosthet Dent. 2012 Mar; 107(3): 170–7.
26. Sorrentino R, Navarra CO, Di Lenarda R, Breschi L, Zarone F, Cadenaro M, et al. Effects of Finish Line Design and Fatigue Cyclic Loading on Phase Transformation of Zirconia Dental Ceramics: A Qualitative Micro-Raman Spectroscopic Analysis. Materials. 2019 Mar 14; 12(6): 863.
27. Camposilvan E, Leone R, Gremillard L, Sorrentino R, Zarone F, Ferrari M, et al. Aging resistance, mechanical properties and translucency of different yttria-stabilized zirconia ceramics for monolithic dental crown applications. Dent Mater J. 2018 Jun; 34(6): 879–90.
28. Mota YA, Cotes C, Carvalho RF, Machado JPB, Leite FPP, Souza ROA, et al. Monoclinic phase transformation and mechanical durability of zirconia ceramic after fatigue and autoclave aging: MECHANICAL DURABILITY OF ZIRCONIA AFTER AGING. J Biomed Mater Res. 2017 Oct; 105(7): 1972–7.
29. Ferrari M, Vichi A, Zarone F. Zirconia abutments and restorations: From laboratory to clinical investigations. Dent Mater J. 2015 Mar; 31(3): e63–76.
30. Wille S, Zumstrull P, Kaidas V, Jessen LK, Kern M. Low temperature degradation of single layers of multilayered zirconia in comparison to conventional unshaded zirconia: Phase transformation and flexural strength. Journal of the Mechanical Behavior of Biomedical Materials. 2018 Jan; 77: 171–5.
31. Stawarczyk B, Keul C, Eichberger M, Figge D, Edelhoff D, Lümkemann N. Three generations of zirconia: From veneered to monolithic. Part I. Quintessence International. 2017 Apr 18; 48(5): 369–80.
32. Ioannidis A, Park J, Hüsler J, Bomze D, Mühlemann S, Özcan M. An in vitro comparison of the marginal and internal adaptation of ultrathin occlusal veneers made of 3D-printed zirconia, milled zirconia, and heat-pressed lithium disilicate. J Prosthet Dent. 2022 Oct; 128(4): 709–15.
33. Jockusch J, Özcan M. Additive manufacturing of dental polymers: An overview on processes, materials and applications. Dent Mater J. 2020 May 27; 39(3): 345–54.
34. Dewan H. Clinical Effectiveness of 3D-Milled and 3D-Printed Zirconia Prosthesis – A Systematic Review and Meta-Analysis. Biomimetics. 2023 Aug 27; 8(5): 394.
35. Khanlar L, Barmak A, Oh Y, Mendha U, Yared S, Zandinejad A. Marginal and internal discrepancies associated with carbon digital light synthesis additively manufactured interim crowns. J Prosthet Dent. 2023 Jul; 130(1): 108.e1–108.e6.
36. Pang Z, Chughtai A, Sailer I, Zhang Y. A fractographic study of clinically retrieved zirconia-ceramic and metal-ceramic fixed dental prostheses. Dent Mater J. 2015 Oct; 31(10): 1198–206.
37. Kongkiatkamon S, Rokaya D, Kengtanyakich S, Peampring C. Current classification of zirconia in dentistry: an updated review. Peer J. 2023 Jul 14; 11: e15669.
38. Tong H, Tanaka CB, Kaizer MR, Zhang Y. Characterization of three commercial Y-TZP ceramics produced for their High-Translucency, High-Strength and High-Surface Area. Ceram Int. 2016 Jan; 42(1): 1077–85.
39. Arellano Moncayo AM, Peñate L, Arregui M, Giner-Tarrida L, Cedeño R. State of the Art of Different Zirconia Materials and Their Indications According to Evidence-Based Clinical Performance: A Narrative Review. Dent J. 2023 Jan 4; 11(1): 18.
40. Vardhaman S, Borba M, Kaizer MR, Kim D, Zhang Y. Wear behavior and microstructural characterization of translucent multilayer zirconia. Dent Mater J. 2020 Nov; 36(11): 1407–17.
41. Kolakarnprasert N, Kaizer MR, Kim DK, Zhang Y. New multi-layered zirconias: Composition, microstructure and translucency. Dent Mater J. 2019 May; 35(5): 797–806.
42. Alves MFRP, Abreu LG, Klippel GGP, Santos C dos, Strecker K. Mechanical properties and translucency of a multi-layered zirconia with color gradient for dental applications. Ceram Int. 2021; 47: 301–9.
43. Rosentritt M, Preis V, Schmid A, Strasser T. Multilayer zirconia: Influence of positioning within blank and sintering conditions on the in vitro performance of 3-unit fixed partial dentures. J Prosthet Dent. 2022 Jan; 127(1): 141–5.
44. Comino-Garayoa R, Peláez J, Tobar C, Rodríguez V, Suárez MJ. Adhesion to Zirconia: A Systematic Review of Surface Pretreatments and Resin Cements. Materials. 2021 May 22; 14(11): 2751.
45. Scaminaci Russo D, Cinelli F, Sarti C, Giachetti L. Adhesion to Zirconia: A Systematic Review of Current Conditioning Methods and Bonding Materials. Dent J. 2019 Aug 1; 7(3): 74.
46. Sulaiman TA, Altak A, Abdulmajeed A, Rodgers B, Lawson N. Cleaning Zirconia Surface Prior To Bonding: A Comparative Study of Different Methods and Solutions. J Prosthodont. 2022 Mar; 31(3): 239–44.
47. Hajjaj MS, Alzahrani SJ. Effect of Different Cleaning Methods on Shear Bond Strength of Resin Cement to Contaminated Zirconia. Materials. 2022 Jul 21; 15(14): 5068.
48. Noronha MDS, Fronza BM, André CB, De Castro EF, Soto-Montero J, Price RB, et al. Effect of zirconia decontamination protocols on bond strength and surface wettability. J Esthet Restor Dent. 2020 Jul; 32(5): 521–9.
49. Ivoclar Vivadent A. Ivoclean: Scientific Documentation. 2011.
50. Tian F, Londono J, Villalobos V, Pan Y, Ho HX, Eshera R, et al. Effectiveness of different cleaning measures on the bonding of resin ce-

ment to saliva-contaminated or blood-contaminated zirconia. J Dent. 2022 May; 120: 104084.
51. Yenisey M, Dede DÖ, Rona N. Effect of surface treatments on the bond strength between resin cement and differently sintered zirconium-oxide ceramics. J Prosthodont Res. 2016 Jan; 60(1): 36–46.
52. Zhang Y, Lawn BR, Rekow ED, Thompson VP. Effect of sandblasting on the long-term performance of dental ceramics. J Biomed Mater Res. 2004 Nov 15; 71B(2): 381–6.
53. Alammar A, Blatz MB. The resin bond to high-translucent zirconia – A systematic review. J Esthet Restor Dent. 2022 Jan; 34(1): 117–35.
54. Ozcan M. Air Abrasion of Zirconia Resin-bonded Fixed Dental Prostheses Prior to Adhesive Cementation: Why and How? J Adhes Dent. 2013 Aug 7; 15(4): 394–394.
55. Blatz MB, Alvarez M, Sawyer K, Brindis M. How to Bond Zirconia: The APC Concept. Compend Contin Educ Dent. 2016 Oct; 37(9): 611–7; quiz 618.
56. Khanlar LN, Takagaki T, Abdou A, Inokoshi M, Ikeda M, Takahashi A, et al. Effect of Air-Particle Abrasion Protocol and Primer on The Topography and Bond Strength of a High-Translucent Zirconia Ceramic. J Prosthodont. 2022 Mar; 31(3): 228–38.
57. Mehari K, Parke AS, Gallardo FF, Vandewalle KS. Assessing the Effects of Air Abrasion with Aluminum Oxide or Glass Beads to Zirconia on the Bond Strength of Cement. J Contemp Dent Pract. 2020 Jul 1; 21(7): 713–7.
58. Khan AA, Mohamed BA, Mirza EH, Syed J, Divakar DD, Vallittu PK. Surface wettability and nano roughness at different grit blasting operational pressures and their effects on resin cement to zirconia adhesion. Dent Mater J. 2019 May 29; 38(3): 388–95.
59. Nagaoka N, Yoshihara K, Tamada Y, Yoshida Y, Meerbeek BV. Ultrastructure and bonding properties of tribochemical silica-coated zirconia. Dent Mater J. 2019 Jan 28; 38(1): 107–13.
60. Sciasci P, Abi-Rached FO, Adabo GL, Baldissara P, Fonseca RG. Effect of surface treatments on the shear bond strength of luting cements to Y-TZP ceramic. J Prosthet Dent. 2015 Mar; 113(3): 212–9.
61. Aboushelib MN. Fusion Sputtering for Bonding to Zirconia-based Materials. J Adhes Dent. 2012 Aug 15; 14(4): 323–8.
62. Ali N, Safwat A, Aboushelib M. The effect of fusion sputtering surface treatment on microshear bond strength of zirconia and MDP-containing resin cement. Dent Mater J. 2019 Jun; 35(6): e107–12.
63. Ma G. Bonding to Zirconia (A Systematic Review). OAJDS [Internet]. 2016 [cited 2023 Dec 3]; 1(1). Available from: https://medwinpublishers.com/OAJDS/OAJDS16000102.php?id=14.
64. Abdelnaby M, El-Etreby A, Aboushelib M, Abdelghany O. Effect of Different Surface Treatments on Bond Strength to Tetragonal and Cubic Zirconia. Futur Dent J. 2020 Jul 1; 6.
65. Çakırbay Tanış M, Akay C, Şen M. Effect of selective infiltration etching on the bond strength between zirconia and resin luting agents. J Esthet Restor Dent. 2019 May; 31(3): 257–62.
66. Aboushelib MN, Kleverlaan CJ, Feilzer AJ. Selective infiltration-etching technique for a strong and durable bond of resin cements to zirconia-based materials. J Prosthet Dent. 2007 Nov; 98(5): 379–88.
67. Saade J, Skienhe H, Ounsi H, Matinlinna JP, Salameh Z. Evaluation of The Effect of Different Surface Treatments, Aging and Enzymatic Degradation on Zirconia-Resin Micro-Shear Bond Strength. CCIDE. 2020 Jan; Volume 12: 1–8.
68. Salem R, Naggar GE, Aboushelib M, Selim D. Microtensile Bond Strength of Resin-bonded Hightranslucency Zirconia Using Different Surface Treatments. J Adhes Dent. 2016 Jun 23; 18(3): 191–6.
69. Esteves-Oliveira M, Jansen P, Wehner M, et al. Surface Characterization and Short-term Adhesion to Zirconia after Ultra-short Pulsed Laser Irradiation. J Adhes Dent. 2017 Jan 3; 18(6): 483–92.
70. Tzanakakis EGC, Beketova A, Papadopoulou L, Kontonasaki E, Tzoutzas IG. Novel Femto Laser Patterning of High Translucent Zirconia as an Alternative to Conventional Particle Abrasion. Dent J. 2021 Feb 8; 9(2): 20.
71. Ghoveizi R, Parsirad R, Tavakolizadeh S, Beyabanaki E. Effect of Different Nd: YAG Laser Power Outputs on Bond Strength of Resin Cement to Zirconia in Comparison to Sandblasting. J Lasers Med Sci. 2021 Feb 16; 12: e6.
72. Saleh N, Guven M, Yildirim G, Erol F. Effect of different surface treatments and ceramic primers on shear bond strength of self-adhesive resin cement to zirconia ceramic. Niger J Clin Pract. 2019; 22(3): 335.
73. Yoshida K. Influence of cleaning methods on resin bonding to saliva-contaminated zirconia. J Esthet Restor Dent. 2018 May; 30(3): 259–64.
74. Lee Y, Oh KC, Kim NH, Moon HS. Evaluation of Zirconia Surfaces after Strong-Acid Etching and Its Effects on the Shear Bond Strength of Dental Resin Cement. Int J Dent. 2019 Jul 1; 2019: 1–8.
75. Mavroudakis E, Cuccato D, Moscatelli D. Determination of Reaction Rate Coefficients in Free-Radical Polymerization Using Density Functional Theory. In: Computational Quantum Chemistry [Internet]. Elsevier; 2019 [cited 2023 Apr 12]: p. 47–98.
76. Carrilho E, Cardoso M, Marques Ferreira M, Marto C, Paula A, Coelho A. 10-MDP Based Dental Adhesives: Adhesive Interface Characterization and Adhesive Stability – A Systematic Review. Materials. 2019 Mar 7; 12(5): 790.
77. Güth JF, Stawarczyk B, Edelhoff D, Liebermann A. Zirconia and its novel compositions: What do clinicians need to know? Quintessence Int. 2019 Jun 14; 50(7): 512–20.
78. Ghodsi S, Arzani S, Shekarian M, Aghamohseni M. Cement selection criteria for full coverage restorations: A comprehensive review of literature. J Clin Exp Dent. 2021; e1154–61.

Neonatal Jaundice: A Study of the Incidence in Children of Rh (D) Negative and 0 Rh (D) Positive Mothers

Josef Urbanec[1,2,*], Kateřina Chládková[3,4], Magdalena Chvílová Weberová[2], Sylva Skálová[5], Jan Kremláček[1,4]

ABSTRACT
Despite advances in neonatal care, neonatal jaundice remains a common problem in maternity wards. The present retrospective epidemiological study collected data on a sample of 710 newborns and compared the incidence of neonatal jaundice in infants born to Rh (D) negative and 0 Rh (D) positive mothers. The primary aim was to determine whether the higher incidence of maternal alloimmunisation in newborns was causally related to a potentially higher incidence of neonatal jaundice in newborns of 0 Rh (D) positive mothers. To the end, we investigated a possible association between the incidence of neonatal jaundice in 0 Rh (D) positive mothers and the neonatal blood group. The incidence of neonatal jaundice was not found to differ between maternal blood groups. We discuss new preventive measures that may reduce the incidence of neonatal jaundice and thereby reduce the length of hospital stay.

KEYWORDS
neonatal jaundice; AB0 and Rh (D) alloimmunisation; haemolytic disease of the foetus and newborn

AUTHOR AFFILIATIONS
[1] Department of Pathological Physiology, Faculty of Medicine in Hradec Králové, Charles University, Czech Republic
[2] Paediatrics Department, Havlíčkův Brod Hospital, Czech Republic
[3] Institute of Psychology, Czech Academy of Sciences, Czech Republic
[4] Department of Medical Biophysics, Faculty of Medicine in Hradec Králové, Charles University, Czech Republic
[5] Paediatrics Department of University Hospital in Hradec Králové, Charles University, Czech Republic
* Corresponding author: Paediatrics Department, Havlíčkův Brod Hospital, Czech Republic; e-mail: josef.urbanec@onhb.cz

Received: 15 February 2024
Accepted: 29 July 2024
Published online: 22 October 2024

Acta Medica (Hradec Králové) 2024; 67(2): 46–52
https://doi.org/10.14712/18059694.2024.19

SUMMARY

Neonatal jaundice is a common diagnosis in the neonatal period, occurring in more than half of all newborns. Most cases represent the physiological postnatal jaundice that does not threaten the life or development of the child and resolves spontaneously. Less commonly, early onset of jaundice is a symptom of a condition that can threaten the newborn's health. A typical example is haemolytic disease of the foetus and newborn. In this article we report a retrospective epidemiological study of over seven hundred newborn babies. We compared the incidence of neonatal jaundice between maternal blood groups with negative Rh (D) factor and mothers with blood group 0 Rh (D) positive and the incidence of maternal alloimmunisation. This study didn't confirm statistically significant differences in the incidence of neonatal jaundice between newborns of Rh (D) negative and 0 Rh (D) positive mothers (P = 0.292). The incidence of alloimmunisation was also comparable in both groups of newborns. These results confirm the need to monitor 0 Rh (D) positive mothers during pregnancy and their newborns after delivery to prevent the development of severe neonatal jaundice. This practice is already common and standard in most neonatal units.

INTRODUCTION

Neonatal jaundice affects almost half of all newborns and is one of the most common problems in all neonatal units (1). Jaundice becomes visible at a serum bilirubin level of 60–80 μmol/L and above. Typical symptoms include yellow skin and mucous membranes, scleral discolouration, poor feeding and excessive sleepiness (1–3). Bilirubin is the product of haemoglobin metabolism from the accelerated breakdown of fetal red blood cells (RBCs). Unconjugated (free, indirectly reactive) bilirubin is a hydrophobic molecule that is normally bound to plasma albumin and transported to the liver. In hepatocytes, bilirubin is bound to glucuronic acid by glucuronosyltransferase. Conjugated (directly reactive) bilirubin is excreted in the bile and passed into the small intestine (see Figure 1) (4). Based on these findings, a distinction can be made between unconjugated and conjugated hyperbilirubinemia. The study reported in this article deals only with unconjugated hyperbilirubinemia.

The most common cause of hyperbilirubinemia in newborns is physiological postnatal jaundice. Its onset usually peaks on the second or third day after birth. It is influenced by several factors, most importantly by an increased number of fetal RBCs and therefore a higher haematocrit. Fetal RBCs are developmentally adapted to a lower partial pressure of oxygen in the blood. After birth, the partial pressure of oxygen is increased, causing the RBCs to degrade more rapidly and the serum bilirubin level to rise. The hepatobiliary system is also less mature in neonates than in adults (1). Several studies have examined the effect of early initiation of breastfeeding in reducing the risk of neonatal jaundice, suggesting that it may reduce neonatal weight loss after birth (5).

The onset of jaundice in the first hours after birth is always pathological. It may be an early symptom of several

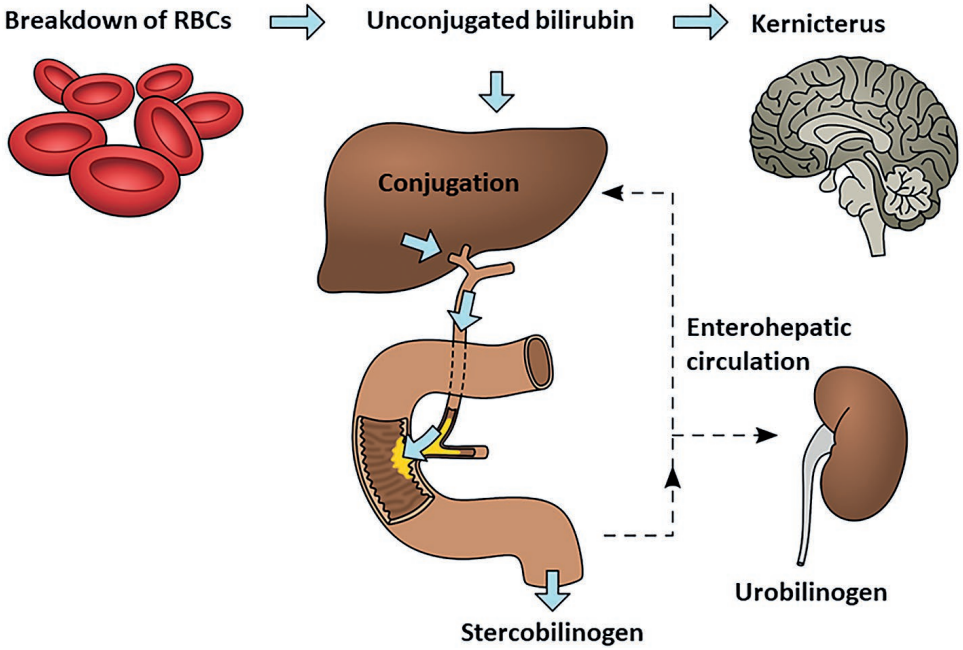

Fig. 1 Bilirubin metabolism and excretion. Haemoglobin and other haem proteins are released from the breakdown fetal red blood cells (RBCs). Unconjugated bilirubin is bound to albumin and transported to the liver. When the albumin binding capacity is saturated, unconjugated bilirubin can cross the blood-brain barrier and can form deposits (core icterus). In hepatocytes the bilirubin is conjugated with glucuronic acid. Conjugated bilirubin is water-soluble and excreted into the bile and passed into the small intestine. Bacterial oxygenation converts bilirubin into urobilinogen and stercobilinogen, which stains the stool. Part of conjugated bilirubin or urobilinogen are reabsorbed by the enterohepatic circulation. Scheme adopted and freely modified from Lissauer T, Clayden G. Neonatal medicine. In: Illustrated Textbook of Paeditrics. 4th edition. Mosby, Elsevier; 2011: 168–172.

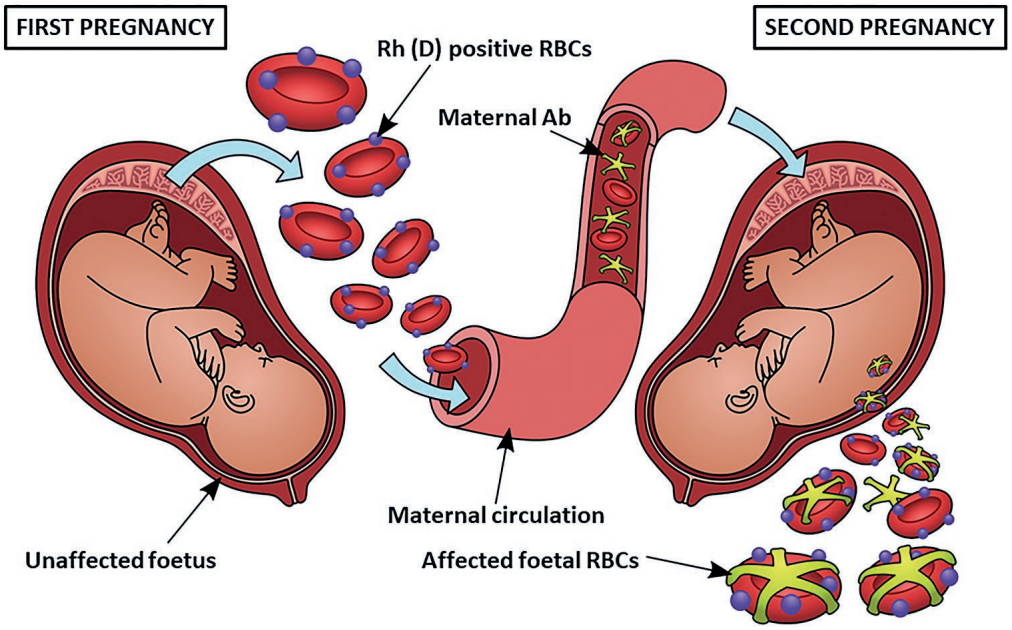

Fig. 2 Scheme of the maternal alloimmunisation and transplacental transfer of antibodies. Typically, the immune system of a Rh (D) negative mother, or less commonly a 0 Rh (D) positive mother, is stimulated by a previous fetomaternal haemorrhage and can produce antibodies. The IgG immunoglobulins cross the placental barrier, enter the fetal circulation during the next pregnancy and bind to the fetal red blood cells (RBCs), causing severe haemolysis. RBCs with bound antibodies are destroyed in the reticuloendothelial system. Scheme adapted and freely modified from MedlinePlus [Internet]. Bethesda (MD): National Library of Medicine (US); Hemolytic disease of the newborn [reviewed 2023 Dec 31]. Available from: https://medlineplus.gov/ency/article/001298.htm.

diseases (e.g. early infection, inborn errors of metabolism, spherocytosis). In this article, we focus on the epidemiology of haemolytic disease of the foetus and newborn (HDFN), excluding other causes of hyperbilirubinemia. HDFN was described in 1941 by the immunohaematologist Phillip Levin and his colleagues on the basis of maternal alloimmunisation (6). The key factor in the pathophysiology of the alloimmune response is the Rhesus (Rh) factor. The Rh factor is an inherited protein of RBCs that is determined by several antigens. The most important is antigen D. Its presence is called Rh (D) positive and its absence Rh (D) negative. Antigen D is a powerful immunological stimulant (7). The immune system of the Rh (D) negative mother is stimulated after a previous pregnancy or abortion of the Rh (D) positive newborn/foetus (when even minimal fetal haemorrhage occurs) and produces antibodies. These immunoglobulins cross the placental barrier and enter the fetal circulation during the next pregnancy and bind to Rh (D) positive fetal RBCs (see Figure 2). In rare cases, maternal alloimmunisation can be caused by an incorrectly administered transfusion or invasive diagnostic procedures – amniocentesis, chorionic villus sampling (8, 9). RBCs with bound antibodies are increasingly taken up and destroyed in the reticuloendothelial system. The resulting fetal anaemia can lead to tachycardia, fetal hydrops and even miscarriage if not treated appropriately (see Figure 3) (6). Classical HDFN is mostly described in Rh (D) negative mothers, but up to 25% of severe cases of HDFN occur in Rh (D) positive mothers. In newborns of 0 Rh (D) positive mothers, it has been suggested that different neonatal blood groups may result in different levels of antigenic stimulation. This stimulation could lead to increased antibody production. A higher incidence of maternal alloimmunisation can be expected, especially in neonates with blood groups A and B (10, 11). The high incidence can also be attributed to other types of Rh antibodies, such as anti-c. As mentioned above, the incidence of severe HDFN caused by incompatibility in the ABO blood system is comparable to the incidence of HDFN caused by Rh incompatibility. In the case of fetal-maternal blood group incompatibility, IgM antibodies are produced which cannot cross the placental barrier due to their pentameric molecular structure. However, some women produce IgG antibodies (namely IgG anti-A haemolysin antibodies in blood group A children and IgG anti-B haemolysin antibodies in blood group B children) which can cross the placental barrier and cause immune haemolysis of RBCs. Taking this mechanism into account, a higher incidence of maternal alloimmunisation or HDFN can be expected in children born to 0 Rh (D) positive mothers (3).

In HDFN, unconjugated hyperbilirubinemia can rise to levels that significantly exceed the binding capacity of plasma proteins. Bilirubin crosses the blood-brain barrier in excess, and bilirubin encephalopathy may develop, with deposits mainly in the basal ganglia and midbrain. If treatment is not started (phototherapy, intravenous immunoglobulins or, in extreme cases, exchange transfusion), the brain damage may become permanent. This is also known as kernicterus (8). The main treatment method used today is phototherapy. This involves using a lamp that emits the blue-green spectrum of visible light (wavelengths 430–490 nm). The light disrupts the structure of bilirubin, facilitating its metabolism and removal. For the first-line treatment of mild hyperbilirubinemia, a lamp or bili-bed is used. This is called general or conventional phototherapy. When the bilirubin level rises to the threshold

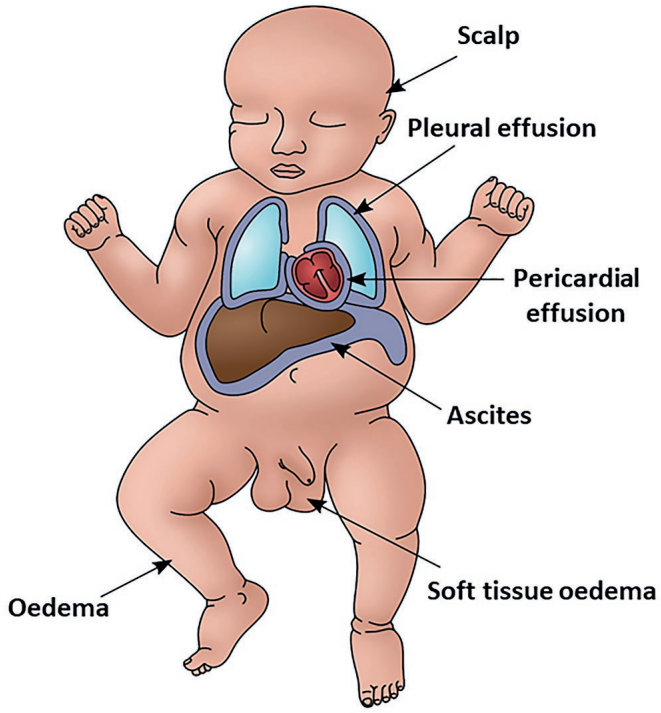

Fig. 3 Hydrops foetalis. Increased destruction of fetal RBCs may result in anaemia. Severe anaemia can cause tachycardia and even heart failure associated with pericardial and pleural effusion, ascites, and skin oedema. All these symptoms are part of hydrops foetalis. If the anaemia is not adequately treated, it may lead to miscarriage.

for exchange transfusion, second-line treatment is indicated, which is intensive phototherapy. This method uses two lamps with the same light characteristics. The irradiance of the light measured on the baby's skin below the centre of the phototherapy lamps is stronger compared to conventional phototherapy.

NEWBORNS COHORT AND METHODS

This paper presents a retrospective epidemiological study of newborns. Clinical and laboratory data were collected at the neonatal department of the Havlíčkův Brod Hospital between 12/2020 and 6/2022. These data were then statistically processed, i.e. the incidence in different groups was evaluated with the χ^2 test. The study group included 710 newborns born to mothers with blood groups A, B, AB, 0 Rh (D) negative and mothers with 0 Rh (D) positive. This selection of newborns is based on the screening of Rh (D) negative mothers to prevent the development of HDFN in subsequent pregnancies. The introduction of blood group testing of newborns of 0 Rh (D) positive mothers was prompted by the increased incidence of HDFN. Blood groups are not routinely tested in newborns of A and B Rh (D) positive mothers. Although HDFN can also occur in these infants, maternal alloimmunisation is less common. Therefore, investigation would be costly and, with current medical knowledge, would not allow intervention in the planning of the next pregnancy.

Inclusion criteria for the participants were: birth in the 36th week of gestation and later, no severe peripartum hypoxia (Apgar score in the first minute 5 points and above), no medication except the usual prophylaxis with vitamin K (1). Laboratory investigations of each participant after delivery from umbilical cord blood sample consisted a blood group, total umbilical bilirubin (μmol/L) and direct antiglobulin test (DAT). These tests should be standard in neonatal care. The diagnostic criteria for HDFN in this study were a positive umbilical PAT, anaemia in the first postnatal blood sample (haemoglobin 140g/L and below), and jaundice requiring phototherapy treatment. We did not monitor the occurrence of concomitant neonatal injuries such as cephalohaematoma, which can increase hyperbilirubinemia levels and cause severe neonatal jaundice. These injuries are common in newborns with delayed adaptation after birth, which were not included in this study.

The incidence of neonatal hyperbilirubinemia was assessed using a transcutaneous bilirubinometer, usually twice a day until discharge. More frequent transcutaneous monitoring was indicated by the paediatrician, especially in newborns with elevated umbilical bilirubin or positive DAT. Elevated umbilical or transcutaneous bilirubin levels above the cut-off value prompted subsequent serum bilirubin testing. Hodr-Poláček charts were used to assess hyperbilirubinemia. These charts were historically used in this department. Nowadays they are replaced by charts of the American Academy of Pediatrics (AAP) recommended by the Czech Society of Neonatology. As mentioned above, children born to A and B Rh (D) positive mothers were not included because the blood group of these children is not routinely checked. Their blood groups are only tested if there is a suspicion of HDFN. This could distort the incidence of HDFN.

RESULTS

710 healthy newborns were included in this study. The mean gestational age at birth was $39^{3/7}$ weeks (from 36 to 42 weeks of gestation). The mean birth weight was 3425 grams (minimum 2300 g, maximum 4630 g), the mean birth length was 50 centimetres (minimum 44 cm, maximum 55 cm). The average Apgar score was 9 points in the first minute and 10 points in the fifth and tenth minutes. As shown in the bottom three rows of Table 1, out of a total of 710 newborns, 137 were children of Rh (D) negative mothers (19.3%) and 573 were children of 0 Rh (D) positive mothers (80.7%). Both groups of newborns had similar characteristics. There were no statistically significant differences in the characteristics of neonates born to Rh (D) negative and 0 Rh (D) positive mothers.

Serum bilirubin was elevated above the physiological limit according to the charts in 85 infants for whom phototherapy was indicated. 20 of these newborns had Rh (D) negative mothers and the remaining 65 newborns had 0 Rh (D) positive mothers (see Table 1). The mean duration of phototherapy was almost the same in both groups, 47 and 47.4 hours, respectively. The incidence of alloimmunisation (positive umbilical DAT) was comparable in both groups of neonates (see Table 2). The incidence of hyperbilirubinemia in the newborns of Rh (D) negative and 0 Rh (D) positive mothers was compared using the

Tab. 1 Incidence of neonatal jaundice (indexed by indication for phototherapy) in the sample of 710 newborns, split by maternal Rh (D): Rh (D) negative pooled across maternal blood groups 0, A, B, AB, and Rh (D) positive pooled across maternal blood group 0.

Phototherapy		Maternal Rh (D) factor		Total
		N	P	
Yes	Observed	20	65	85
	% within row	23.5%	76.5%	100.0%
	% within column	14.6%	11.3%	12.0%
Nop	Observed	117	508	625
	% within row	18.7%	81.3%	100.0%
	% within column	85.4%	88.7%	88.0%
Total	Observed	137	573	710
	% within row	19.3%	80.7%	100.0%
	% within column	100.0%	100.0%	100.0%

Tab. 2 Incidence of neonatal jaundice (indexed by indication for phototherapy) in the sample of 710 newborns, split by neonatal blood group and maternal Rh (D).

Neonatal blood group	Rh (D) mother	Phototherapy indicated		Total
		No	Yes	
0	N	48	7	55
	P	296	25	321
	Total	344	32	376
A	N	50	5	55
	P	144	28	172
	Total	194	33	227
AB	N	3	3	6
	P	0	0	0
	Total	3	3	6
B	N	16	5	21
	P	68	12	80
	Total	84	17	101
Total	N	117	20	137
	P	508	65	573
	Total	625	85	710

χ^2 test. The test showed no statistically significant difference in the incidence of neonatal jaundice between Rh (D) negative and 0 Rh (D) positive mothers (χ^2 = 1.111, df = 1, P= 0.292).

In a more detailed analysis of the 65 children of 0 Rh (D) positive mothers, maternal alloimmunisation was detected in 22 newborns. 7 newborns had bilirubin levels above the threshold for intensive phototherapy. Maternal antibodies (positive umbilical DAT) were confirmed in 5 of these 7 newborns. For comparison, 2 infants of Rh (D) negative mothers were indicated for intensive phototherapy and both infants were DAT positive (see Table 3). This therapy was successful in all cases. There was only one newborn of a 0 Rh (D) positive mother who met the

Tab. 3 Incidence of common and intensive phototherapy compared with maternal alloimmunisation in neonates born to 0 Rh (D) positive and all Rh (D) negative mothers. Positive maternal alloimmunisation is similar in both groups.

Maternal blood group	Phototherapy indicated in newborns		
	Common	Intensive	Total
0 Rh (D) positive	58	7	65
	Maternal alloimmunisation (DAT) positive		
	17	5 (71%)	22 (33.8%)
All Rh (D) negative	18	2	20
	Maternal alloimmunisation (DAT) positive		
	4	2 (100%)	6 (30%)

criteria for HDFN (ABO incompatibility). The incidence of HDFN in this study was 0.14% of all newborns and 1.17% of newborns with neonatal jaundice for whom phototherapy was indicated, respectively. Despite proven alloimmunisation, no neonates with severe haemolytic anaemia requiring transfusion, administration of IVIG or exchange transfusion were reported.

The sample was also characterised according to neonatal blood group, based on our assumption that different neonatal blood groups could lead to differences in the strength of antigenic stimulation (10, 11). Table 4 shows the incidence of neonatal jaundice responding to phototherapy according to neonatal blood group and maternal blood group.

The incidence of jaundice in newborns of Rh (D) negative versus 0 Rh (D) positive mothers, by neonatal blood

Tab. 4 Incidence of neonatal jaundice (indexed by indication for phototherapy) in the sample of 710 newborns, subdivided by neonatal blood group and maternal Rh (D). The percentages show the incidence of jaundice for each subgroup compared to the total number of children.

Neonatal blood group	Maternal Rh (D)	Phototherapy indicated		Total
		No	Yes	
0	N	48	7 (12.7%)	55
	P	296	25 (7.8%)	321
	Total	344	32	376
A	N	50	5 (9.0%)	55
	P	144	28 (16.2%)	172
	Total	194	33	227
AB	N	3	3 (50.0%)	6
	P	0	0 (0.0%)	0
	Total	3	3	6
B	N	16	5 (23.8%)	21
	P	68	12 (15.0%)	80
	Total	84	17	101
Total	N	117	20 (14.6)	137
	P	508	65 (11.3)	573
	Total	625	85	710

Tab. 5 Incidence of neonatal jaundice (indexed by indication for phototherapy) in the sample of 710 newborns, split by neonatal blood group and maternal Rh (D). The abbreviation NaN (Not a Number) stands for no number.

Neonatal blood group		Value	df	p
0	χ^2	1.47	1	0.2252
	N	376		
A	χ^2	1.73	1	0.1880
	N	227		
AB	χ^2	NaN	1	NaN
	N	6		
B	χ^2	0.92	1	0.3369
	N	101		
Total	χ^2	1.11	1	0.2918
	N	710		

group, was tested using separate χ^2 tests. For none of the newborn blood groups did the tests detect a statistically significant difference between the incidence in newborns of Rh (D) negative versus 0 Rh (D) positive mothers (see Table 5). Therefore, we cannot conclude that there is an association between the development of neonatal jaundice and the blood groups of mothers and newborns. This null result should be interpreted with caution, as the lack of effect could be due to the small number of children represented especially for newborns blood type AB (only 3 newborns in this subgroup). However, given the caveats about interpreting null effects (where failure to detect an effect does not mean that the effect does not exist), further research with larger samples is needed to better understand the relationship between maternal Rh (D), neonatal blood group and the incidence of neonatal jaundice.

DISCUSSION

Before the introduction of prophylaxis in Rh (D) negative mothers with anti-D antibodies (introduced in the former Czechoslovakia in the 1980s), the worldwide incidence of HDFN was about 1% of all newborns and the mortality rate reached the level of 50% (12, 13). With the introduction of prophylaxis, the incidence of HDFN in newborns of Rh (D) negative mothers has decreased to about 0.5%. Nowadays, the incidence of Rh (D) and ABO alloimmunisation is similar (14). In our study, the incidence of ABO alloimmunisation was present in approximately 1% of ABO mismatched pregnancies. The results of our study correlate with other reviewed studies – the incidence of maternal alloimmunisation was not found to differ between the studied groups of newborns (10). These results don't support the initial hypothesis of a higher incidence of neonatal jaundice in newborns of 0 Rh (D) positive mothers. It's still necessary to continue with the established prophylaxis mentioned above. However, the incidence of neonatal jaundice and ABO alloimmunisation might be higher with extended screening of newborns of all Rh (D) positive mothers.

Because of this incidence, prenatal screening for maternal antibodies to the minor antigens of the Rh factor and other RBC antigens (e.g. anti-C and anti-K) is essential (ref 7, 8, 15–17). Combined first and third trimester screening for these antibodies has already been introduced in several countries (e.g. the Netherlands) to detect alloimmunisation not captured at first trimester screening ("late" alloimmunisation) and subsequent HDFN (8). The results of this screening showed that Rh antibodies were found in 1 in 300 pregnant women. Since 2011, the Czech Republic has introduced first and third trimester screening (at 12 and 28 weeks' of gestation) for numerous maternal antibodies (C, Cw, c, D, E, e, K, k, Fya, Fyb, Jka, Jkb, S, s, M, N, Lea) (18). These antibodies are more common in Rh (D) negative women, but further research may shed new light on the alloimmunisation of newborns of Rh (D) positive mothers. This knowledge would be important as the onset of jaundice caused by alloimmunisation in newborns of 0 Rh (D) positive mothers could be as rapid as in newborns of Rh (D) negative mothers (19). Pathological elevation of umbilical cord bilirubin is also observed, and serum bilirubin may reach higher levels. Possible prevention of new antigens may lead to a reduction in the incidence of HDFN, similar to the previously established anti-D prophylaxis (20). New interventions would reduce neonatal morbidity associated with multiple neonatal jaundice and have also economic benefits. The authors suggest that further research into alloimmunisation in children born to 0 Rh (D) positive mothers would improve the quality of care for neonates born to A and B Rh (D) positive mothers.

CONCLUSION

This study compared the incidence of pathological neonatal jaundice in neonates born to Rh (D) negative and 0 Rh (D) positive mothers. Contrary to our expectations, based on screening practice and universal HDFN prophylaxis in all Rh (D) negative mothers, the predicted higher incidence of jaundice due to maternal alloimmunisation in 0 Rh (D) positive mothers wasn't confirmed. There are no reports in the reviewed literature of similar data prior to the introduction of the now widespread HDFN prophylaxis in Rh (D) negative mothers. In line with the present results, which didn't show a higher incidence of neonatal jaundice in Rh (D) negative compared to Rh (D) positive mothers, we confirm the need to monitor Rh (D) positive mothers and their newborns. However, this practice was introduced in our neonatal units only a few years ago. Its initiation was also the impetus for the conduct of this study.

CONFLICT OF INTEREST STATEMENT

All authors declare no conflicts of interest.

REFERENCES

1. Brits H, Adendorff J, Huisamen D, et al. The prevalence of neonatal jaundice and risk factors in healthy term neonates at National District Hospital in Bloemfontein. Afr J Prim Health Care Fam Med. 2018 Apr 12; 10(1): e1–e6.
2. Straňák Z, Janota J. Neonatolgie. 2nd edition. Praha: Mladá fronta, 2015.

3. Lissauer T, Clayden G. Neonatal medicine. In: Illustrated Textbook of Paeditrics. 4th edition. Mosby, Elsevier, 2011: 168–172.
4. Rennie JM, Kendall G. A manual of Neonatal Intensive Care. 5th edition. Taylor & Francis Ltd, 2013.
5. Ketsuwan S, Baiya N, Maelhacharoenporn K, Puapornpong P. The Association of Breastfeeding Practices with Neonatal Jaundice. J Med Assoc Thai. 2017 Mar; 100(3): 255–61.
6. Koelewijn JM, Vrijkotte TG, van der Schoot CE, Bonsel GJ, de Haas M. Effect of screening for red cell antibodies, other than anti-D, to detect hemolytic disease of the fetus and newborn: a population study in the Netherlands. Transfusion. 2008 May; 48(5): 941–52.
7. Ľubušký M. Prevence Rh (D) aloimunizace u Rh (D) negativních žen. Prakt Gyn. 2008; 12(2): 100–103.
8. Slootweg YM, Koelewijn JM, van Kamp IL, van der Bom JG, Oepkes D, de Haas M. Third trimester screening for alloimmunisation in Rhc-negative pregnant women: evaluation of the Dutch national screening programme. BJOG. 2016 May; 123(6): 955–63.
9. Ullah S, Rahman K, Hedayati M. Hyperbilirubinemia in Neonates: Types, Causes, Clinical Examinations, Preventive Measures and Treatments: A Narrative Review Article. Iran J Public Health. 2016 May; 45(5): 558–68.
10. Thakur AA, Ansari MA, Mishra A, Jha SK. Outcome of Neonatal Jaundice in term neonates with ABO incompatibility at tertiary care center. Int J Contemp Pediatr. 2020 Oct; 7(10): 1973–1977.
11. Kaplan M, Hammerman C, Vreman HJ, Wong RJ, Stevenson DK. Hemolysis and hyperbilirubinemia in antiglobulin positive, direct ABO blood group heterospecific neonates. J Pediatr. 2010 Nov; 157(5): 772–7.
12. Ree IMC, Smits-Wintjens VEHJ, van der Bom JG, van Klink JMM, Oepkes D, Lopriore E. Neonatal management and outcome in alloimmune hemolytic disease. Expert Rev Hematol. 2017 Jul; 10(7): 607–616.
13. Yu D, Ling LE, Krumme AA, Tjoa ML, Moise KJ Jr. Live birth prevalence of hemolytic disease of the fetus and newborn in the United States from 1996 to 2010. AJOG Glob Rep. 2023 Mar 24; 3(2): 100203.
14. Myle AK, Al-Khattabi GH. Hemolytic Disease of the Newborn: A Review of Current Trends and Prospects. Pediatric Health Med Ther. 2021 Oct 7; 12: 491–498.
15. Ľubušký M. Management těhotenství s rizikem rozvoje hemolytické nemoci plodu a novorozence. Postgrad Med. 2016; 18(4): 352–356.
16. De Haas M, Thurik FF, Koelewijn JM, van der Schoot CE. Haemolytic disease of the fetus and newborn. Vox Sang. 2015 Aug; 109(2): 99–113.
17. Martin JA, Hamilton BE, Sutton PD, Ventura SJ, Menacker F, Munson ML. Births: final data for 2002. Natl Vital Stat Rep. 2003 Dec 17; 52(10): 1–113.
18. Dušková D, Kubánková H, Masopust J, Pejchalová A, Písačka M. Imunohematologická vyšetření v těhotenství a po porodu. Transfuze Hematol dnes. 16, 2010, No. 1: 1–20.
19. Kalekheti BK, Singh R, Bhatta NK, Karku A, Baral N. Risk of neonatal hyperbilirubinemia in babies born to 'O' positive mothers: A prospective cohort study. Kathmandu Univ Med J. 2009; 7(1): 11–15.
20. Stetson B, Scrape S, Markham KB. Anti-M Alloimmunization: Management and Outcome at a Single Institution. AJP Rep. 2017 Oct; 7(4): e205–e210.

Impact of Age on Predictive Capabilities of Ferritin, Ferritin-Hemoglobin Ratio, IL-6, and sIL-2R for COVID-19 Severity and Mortality

Oleksii Skakun[1,*], Yaroslava Vandzhura[2], Ihor Vandzhura[2], Khrystyna Symchych[3], Anton Symchych[4]

ABSTRACT

The study aimed to establish the impact of age on the predictive capability of ferritin, ferritin-hemoglobin ratio (FHR), IL-6, and sIL-2R in COVID-19 patients. Compared to patients with moderate condition, patients with severe condition had higher ferritin level (441.0 [188.0–829.8] ng/mL vs 281.0 [172.0–388.0] ng/mL, p = 0.002), sIL-2R level (6.0 [4.7–9.0] pg/mL vs 5.3 [3.7–6.9] pg/mL, p = 0.020), FHR (38.4 [15.1–63.4] vs 22.0 [12.1–32.1], p = 0.002). The area under the curves (AUC) for discriminative capabilities of the following biomarkers for severe condition were assessed in patients aged <65 years and patients aged ≥65 years: ferritin (AUC = 0.585, p = 0.309 vs AUC = 0.683, p = 0.002), FHR (AUC = 0.589, p = 0.302 vs AUC = 0.688, p = 0.002), IL-6 (AUC = 0.503, p = 0.972 vs AUC = 0.647, p = 0.019), and sIL-2R (AUC = 0.549, p = 0.552 vs AUC = 0.646, p = 0.017). Also AUCs for discriminative capabilities for in-hospital mortality were compared in patients aged <65 years and ≥65 years: ferritin (AUC = 0.607, p = 0.628 vs AUC = 0.661, p = 0.105), FHR (AUC = 0.612, p = 0.621 vs AUC = 0.688, p = 0.002), IL-6 (AUC = 0.580, p = 0.724 vs AUC = 0.695, p = 0.016), and sIL-2R (AUC = 0.620, p = 0.491 vs AUC = 0.695, p = 0.029). Thus, ferritin, FHR, IL-6, and sIL-2R didn't show acceptable predictive value for severe condition and lethal outcome in patients aged <65 years but had high predictive value for lethal outcome in patients aged ≥65 years.

KEYWORDS

COVID-19; ferritin; IL-6; soluble IL-2 receptors; age; prediction; severity; mortality

AUTHOR AFFILIATIONS

[1] Clinic of St. Luka, Ivano-Frankivsk, Ukraine
[2] Ivano-Frankivsk National Medical University, Department of Internal Medicine #2 and Nursing, Ivano-Frankivsk, Ukraine
[3] Ivano-Frankivsk National Medical University, Department of Therapy, Family and Emergency Medicine Postgraduate Education, Ivano-Frankivsk, Ukraine
[4] Ivano-Frankivsk National Medical University, Department of General and Vascular Surgery, Ivano-Frankivsk, Ukraine
* Corresponding author: Ivano-Frankivsk city, Mazepy street, 114, Ivano-Frankivsk region, Ukraine; e-mail: olexiy109921@ukr.net

Received: 2 May 2024
Accepted: 15 August 2024
Published online: 22 October 2024

Acta Medica (Hradec Králové) 2024; 67(2): 53–59
https://doi.org/10.14712/18059694.2024.20

INTRODUCTION

COVID-19 pandemic significantly impacted the social, health, and economic spheres of human life (1). According to WHO reports, as of 12 October 2023, there were over 771 million confirmed cases of COVID-19 and almost 7 million deaths related to this disease worldwide (2). Globally, the case-fatality rate is 0.90% (3). Among hospitalized patients, the death rate at 30 days is almost 6.0% (4). However, the full impact of COVID-19 seems to be much more significant, than reported deaths, as excessive mortality is found to be significantly higher (5).

COVID-19 leads to a hyperinflammatory state resulting in lung damage, acute respiratory distress syndrome, as well as multi-organ failure (6). There are multiple biomarkers that reflect systemic inflammation. Serum ferritin is one of them (7–9). Many studies showed that serum ferritin level is a predictor of severe COVID-19 and lethal outcomes (10–13). However, several studies showed that ferritin is an insufficiently accurate predictor of adverse outcomes in patients with COVID-19 (14, 15). Predictive abilities of ferritin-hemoglobin ratio (16), ferritin-lymphocyte percentage ratio (17, 18), and ferritin-albumin ratio (19) were studied to improve ferritin role in the prediction of severe COVID-19 and mortality. Higher predictive accuracy of the abovementioned ratios compared to single ferritin is explained by the fact that severe COVID-19 is accompanied by an increase in ferritin level (20, 21), a decrease in hemoglobin (22) and albumin (23, 24) levels, as well as lymphocyte count (25–27). However, age has a great effect on ferritin levels in COVID-19 patients (28)

Soluble interleukin-2 receptors (sIL-2R) and interleukin-6 (IL-6) are other important predictors of adverse outcomes in patients with COVID-19 (29, 30). It's known that age impacts levels of both IL-6 (31) and sIL-2R (32) too.

Therefore, given that age impacts levels of serum ferritin, IL-6, and sIL-2R, it's important to establish whether age impacts the predictive capability of these biomarkers. So, this study aims to establish the influence of age on the predictive capability of ferritin, ferritin-hemoglobin ratio, IL-6, and sIL-2R in patients hospitalized for pneumonia associated with COVID-19.

MATERIALS AND METHODS

One hundred thirty-five patients hospitalized for pneumonia associated with COVID-19 between March and June 2021 were included in this study. SARS-CoV-2 was confirmed in each patient with PCR or ELISA test (IgM levels). Pneumonia was confirmed in each patient radiologically (either X-ray or chest computed tomography). Levels of ferritin, IL-6, and sIL-2R were assessed at the moment of hospital admission. To calculate the ferritin-hemoglobin ratio, the serum ferritin level (ng/mL) was divided by hemoglobin level (g/dL).

COVID-19 severity was established according to the Protocol of Medical Care of Coronavirus Disease (COVID-19) (33). A severe clinical condition was diagnosed in patients with at least one of the following signs: oxygen saturation ≤93%, respiratory rate ≥30 breaths per minute, and radiologically established pulmonary infiltrates involving >50% of the lung area. The critical clinical condition was established in patients with at least one of the following conditions: altered consciousness (≤14 points according to Glasgow Coma Scale), acute respiratory distress syndrome, sepsis-III criteria, and multiple organ dysfunction syndrome. The moderate clinical condition was diagnosed in COVID-19 patients with pulmonary involvement confirmed radiologically who don't meet criteria of severe or critical clinical conditions.

An informed consent was signed by each potential patient before enrollment into the research. The approval of the Ethics Committee of Ivano-Frankivsk National Medical University (No 134/23) has been acquired. The study has been performed according to the Declaration of Helsinki.

Software MedCalc and MS Excel were used for statistical processing. The distribution of variables was evaluated Shapiro-Wilk test. The variables with abnormal distribution were shown as a median and interquartile range. Categorical variables were presented as a total count accompanied by a corresponding percentage. Mann-Whitney U test, Chi-squared test, and Spearman's rank correlation were used. Receiver operating characteristic (ROC) curves were constructed and the area under the curve (AUC) was computed. Sensitivity, specificity, and Youden index were determined. Also, a comparison of two AUCs was performed. P-values less than 0.05 were considered to be statistically significant.

RESULTS

Participants characteristics. The participants had a median age of 67.0 (61.0–74.0) years. The median value of body mass index in enrolled patients was 27.0 (24.6–31.8) kg/m^2. The median oxygen saturation in patients at the moment of admission was 95.0 (93.0–96.0)%. Among the participants, there were 53 (39.3%) men and 82 (60.7%) women. The median hemoglobin level at the moment of hospital admission was 13.1 (12.2–14.2) g/dL. The median ferritin level at admission was 349.0 (183–595.8) ng/mL. The median ferritin-hemoglobin ratio was 25.7 (13.3–45.8). The median IL-6 level at the moment of hospital admission was 44.4 (13.0–91.8) pg/mL. The median sIL-2R level at the moment of hospital admission was 5.6 (4.2–7.7) ng/mL.

Severe/critical conditions during the in-patient stay developed in 72 (53.3%) patients, and moderate condition was diagnosed in 63 (46.7%) patients. Supplemental oxygen was used in 62 (45.9%) patients. During the in-hospital stay, 14 (10.4%) patients died. Laboratory parameters in accordance with COVID-19 severity and mortality are shown in table 1. Ferritin, ferritin-hemoglobin ratio, and sIL-2R at admission were higher in patients with severe/critical conditions than in patients with moderate conditions. Non-survivors had a higher ferritin-hemoglobin ratio at hospital admission.

Discriminative and predictive capabilities of ferritin, ferritin-hemoglobin ratio, IL-6, and sIL-2R. Discriminative capabilities of ferritin, ferritin-hemoglobin ratio, IL-6, and sIL-2R for severity and mortality are shown in table 2

Tab. 1 Laboratory parameters in the enrolled patients at the moment of hospital admission.

Laboratory parameter	Severity			Mortality		
	Moderate condition	Severe/critical condition	p	Survivors	Non-survivors	P
Hemoglobin, g/dL	130.5 (123.0–140.0)	131.0 (121.0–142.0)	0.986	131.0 (123.5–142.0)	122.0 (112.8–141.5)	0.237
Ferritin, ng/mL	281.0 (172.0–388.0)	441.0 (188.0–829.8)	0.002	337.0 (179.0–549.0)	467.5 (397.0–1008.0)	0.066
FHR	22.0 (12.1–32.1)	38.4 (15.1–63.4)	0.002	24.5 (13.1–44.6)	40.1 (29.9–95.3)	0.047
IL-6, pg/mL	36.2 (8.1–71.4)	56.4 (16.2–105.3)	0.055	40.4 (11.5–81.7)	80.4 (26.8–153.7)	0.063
sIL-2R, ng/mL	5.3 (3.7–6.9)	6.0 (4.7–9.0)	0.020	5.4 (3.9–7.6)	7.1 (5.0–9.5)	0.094

Abbreviations: FHR, ferritin-hemoglobin ratio; IL-6, interleukin-6; sIL-2R, soluble interleukin-2 receptors.

Tab. 2 Discriminative capabilities of laboratory parameters for the disease severity and mortality.

Laboratory parameter	Severity			Mortality		
	AUC	SE	p	AUC	SE	p
Ferritin	0.653	0.049	0.002	0.651	0.087	0.083
FHR	0.658	0.049	0.001	0.668	0.094	0.075
IL-6	0.596	0.049	0.052	0.652	0.078	0.052
sIL-2R	0.616	0.048	0.016	0.637	0.083	0.100

Abbreviations: AUC, area under the curve; FHR, ferritin-hemoglobin ratio; IL-6, interleukin-6; SE, standard error; sIL-2R, soluble interleukin-2 receptors.

and fig. 1. Ferritin, ferritin-hemoglobin ratio, and sIL-2R had poor but statistically significant discriminative capabilities for severe/critical condition.

Optimal cut-off values for the prediction of severe/critical condition and lethal outcome are shown in table 3. Only ferritin and ferritin-hemoglobin ratio had acceptable Youden indexes for the prediction of lethal outcome.

Effect of elderly on predictive capabilities of ferritin, ferritin-hemoglobin ratio, IL-6, and sIL-2R. There were 53 (39.3%) patients aged <65 years and 82 (60.7%) patients aged ≥65 years. There was no statistically significant difference between participants aged <65 years and participants aged ≥65 years in ferritin level, ferritin-hemoglobin ratio, IL-6, sIL-2R (table 4).

Correlation analysis between the age and laboratory parameters was performed. There was no correlation between age and ferritin level (r = 0.116, p = 0.182), ferritin-hemoglobin ratio (r = 0.140, p = 0.110), IL-6 level

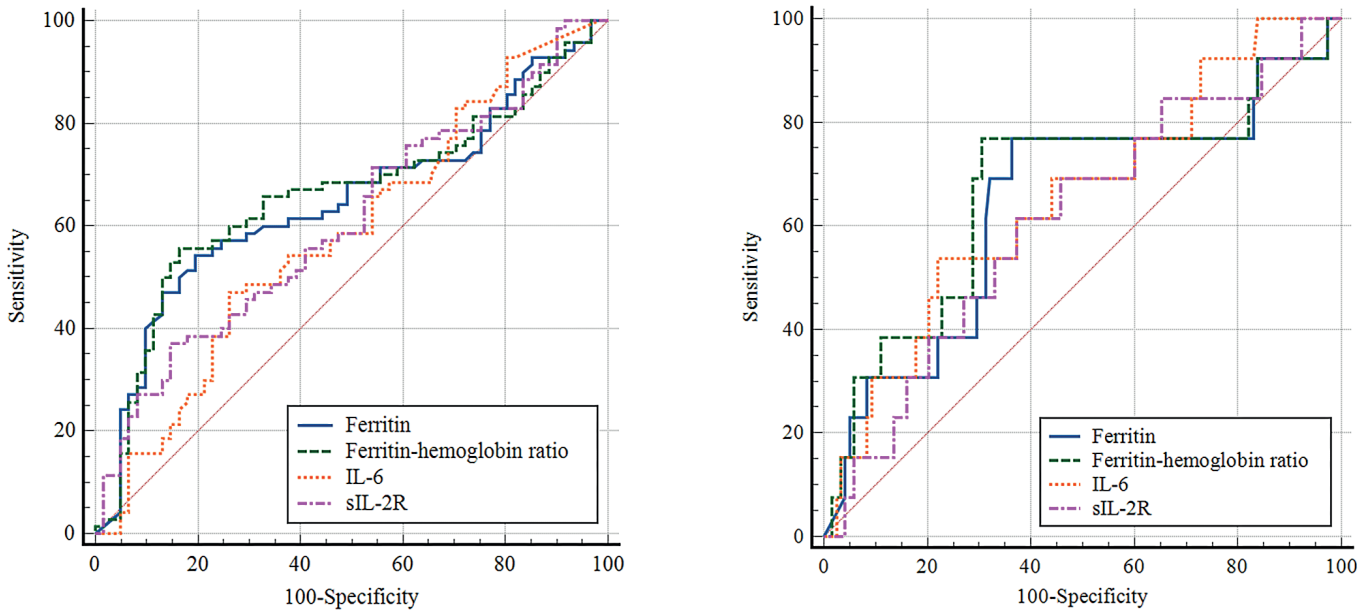

Fig. 1 ROC-curves of discriminative capabilities of ferritin, ferritin-hemoglobin ratio, IL-6, and sIL-2R for severe/critical condition (A) and lethal outcome (B).

Tab. 3 Predictive capabilities of laboratory parameters for the disease severity and mortality.

Laboratory parameter	Severe/critical condition				Lethal outcome			
	Optimal cut-off value	Sensitivity, %	Specificity, %	Youden index	Optimal cut-off value	Sensitivity, %	Specificity, %	Youden index
Ferritin	402.0	54.9	80.6	0.356	396.0	78.6	63.9	0.425
FHR	34.0	55.7	83.6	0.393	35.2	76.9	69.5	0.464
IL-6	62.5	48.6	74.6	0.232	91.0	50.0	77.7	0.277
sIL-2R	7.5	38.9	85.7	0.246	6.2	64.3	62.8	0.271

Abbreviations: FHR, ferritin-hemoglobin ratio; IL-6, interleukin-6; sIL-2R, soluble interleukin-2 receptors.

Tab. 4 Laboratory parameters in patients aged <65 years and patients aged ≥65 years.

Laboratory parameter	Patients aged <65 years	Patients aged ≥65 years	p
Ferritin, ng/mL	285.0 (164.0–549.0)	378.5 (202.5–618.5)	0.336
FHR	22.5 (12.2–43.8)	29.5 (15.5–46.4)	0.284
IL-6, pg/mL	29.9 (11.7–68.8)	56.1 (16.1–98.3)	0.190
sIL-2R, ng/mL	5.1 (3.6–7.3)	5.7 (4.5–8.2)	0.100

Abbreviations: FHR, ferritin-hemoglobin ratio; IL-6, interleukin-6; sIL-2R, soluble interleukin-2 receptors.

(r = 0.154, p = 0.074). A weak but significant positive correlation was seen between age and sIL-2R level at admission (r = 0.230, p = 0.007).

Severe/critical condition was established in 48 (58.5%) patients aged ≥65 years and 24 (45.2%) patients aged <65 years (p = 0.133). 11 (13.4%) patients aged ≥65 years and 3 (5.7%) patients aged <65 years died during in-patient stay (p = 0.151).

Discriminative and predictive capabilities of ferritin, ferritin-hemoglobin ratio, IL-6, and sIL-2R for severe/critical condition and lethal outcomes in patients aged <65 years and patients aged ≥65 years are shown in table 5 and fig. 2. Each laboratory parameter failed to show acceptable discriminative capability for the disease severity and in-hospital mortality in patients aged <65 years. However, ferritin, ferritin-hemoglobin ratio, IL-6, and sIL-2R showed weak discriminative capabilities for the disease severity in patients aged ≥65 years. Ferritin-hemoglobin ratio, IL-6, and sIL-2R had acceptable discriminative capabilities with an acceptable Youden index for in-hospital mortality in patients aged ≥65 years. However, there was no statistical significance comparing AUCs for discriminative capabilities of ferritin, ferritin-hemoglobin ratio, IL-6, and sIL-2R in patients aged ≥65 years and patients aged <65 years.

Logistic regression was performed, adjusted and unadjusted odds ratios were calculated (table 6). Unadjusted odds ratio showed that ferritin, ferritin-hemoglobin ratio,

Tab. 5 Discriminative and predictive capabilities of laboratory parameters for severity and mortality in patients aged <65 years and patients aged ≥65 years

Laboratory parameter	<65 years old				≥65 years old				Comparison of two AUCs	
	AUC; SE	p	Optimal cut-off value	Youden index	AUC; SE	p	Optimal cut-off value	Youden index	Difference	p
Severe/critical condition										
Ferritin	0.585; 0.084	0.309	463.0	0.279	0.683; 0.060	0.002	396.0	0.405	0.098	0.342
FHR	0.589; 0.087	0.302	25.6	0.369	0.688; 0.059	0.002	35.2	0.436	0.099	0.346
IL-6	0.503; 0.082	0.972	50.6	0.140	0.647; 0.063	0.019	62.5	0.268	0.144	0.164
sIL-2R	0.549; 0.082	0.552	8.3	0.181	0.646; 0.061	0.017	7.3	0.311	0.097	0.343
Lethal outcome										
Ferritin	0.607; 0.220	0.628	391.0	0.347	0.661; 0.099	0.105	438.0	0.470	0.054	0.823
FHR	0.612; 0.227	0.621	34.3	0.381	0.688; 0.059	0.002	35.2	0.436	0.076	0.746
IL-6	0.580; 0.227	0.724	12.7	0.407	0.695; 0.081	0.016	41.4	0.325	0.115	0.633
sIL-2R	0.620; 0.174	0.491	6.3	0.320	0.695; 0.089	0.029	6.6	0.361	0.075	0.701

Abbreviations: AUC, area under the curve; FHR, ferritin-hemoglobin ratio; IL-6, interleukin-6; SE, standard error; sIL-2R, soluble interleukin-2 receptors.

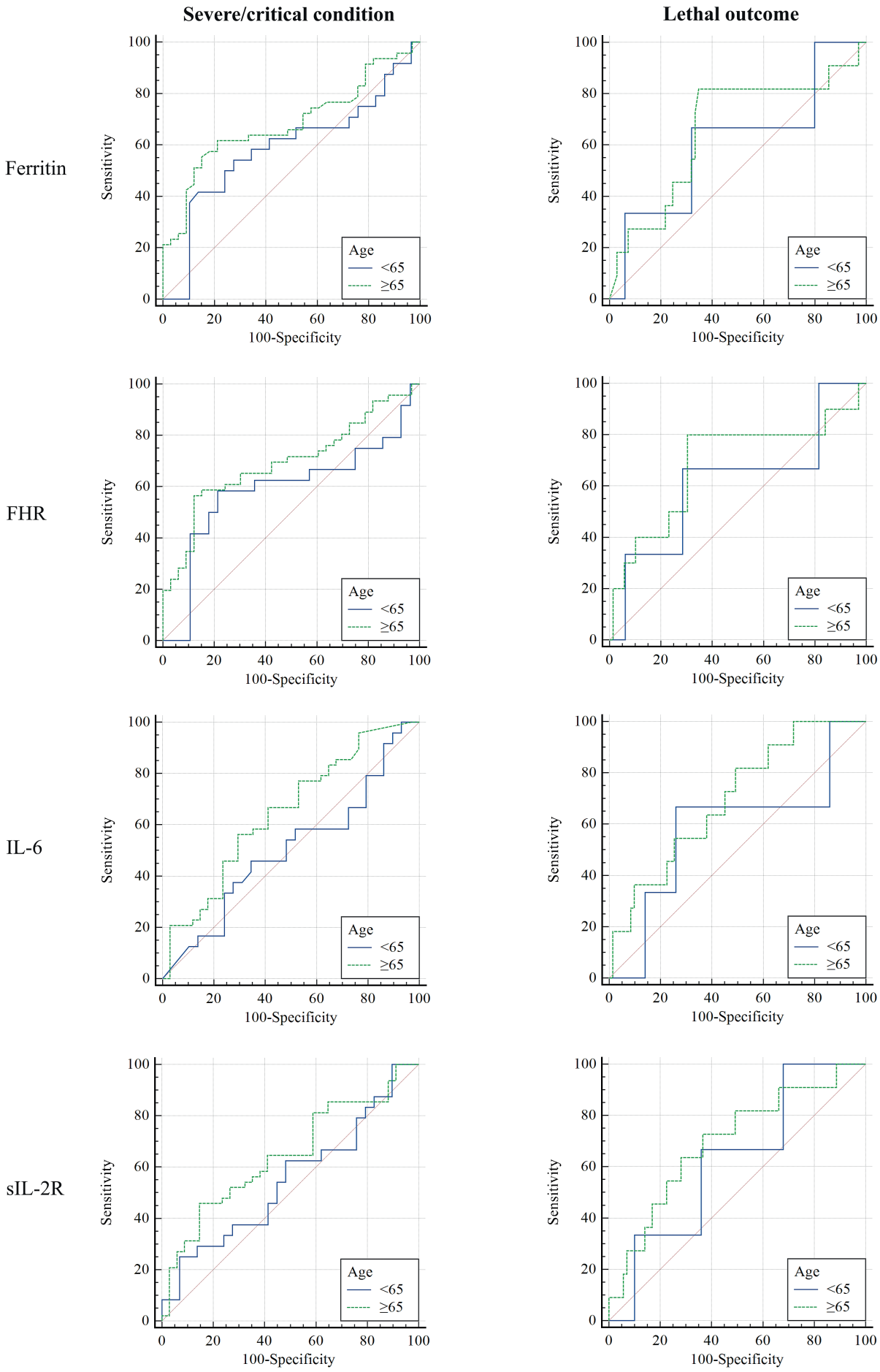

Fig. 2 ROC-curves of discriminative capabilities of ferritin, ferritin-hemoglobin ratio (FHR), IL-6, and sIL-2R for severe/critical condition and lethal outcome in patients aged <65 years and patients aged ≥65 years.

Tab. 6 Odds ratio for prediction of severe/critical clinical condition and lethal outcome in patients aged <65 years and patients aged ≥65 years.

Laboratory parameter	<65 years old		≥65 years old	
	Unadjusted OR (95% CI)	Adjusted OR (95% CI)	Unadjusted OR (95% CI)	Adjusted OR (95% CI)
Severe/critical condition				
Ferritin	1.0001 (0.9995–1.0022)	1.0052 (0.9941–1.0164)	1.0026 (1.0008–1.0045)	1.0016 (0.9960–1.0072)
FHR	1.0094 (0.9911–1.0281)	0.9393 (0.8097–1.0897)	1.0344 (1.0105–1.0589)	1.0093 (0.9391–1.0849)
IL-6	0.9987 (0.9945–1.0030)	0.9986 (0.9937–1.0035)	1.0054 (0.9985–1.0123)	1.0035 (0.9960–1.0110)
sIL-2R	1.1595 (0.9389–1.4318)	1.1149 (0.8820–1.4094)	1.2180 (1.0216–1.4522)	1.1293 (0.9316-1.3688)
Lethal outcome				
Ferritin	1.0009 (0.9983–1.0034)	0.9926 (0.9767–1.0087)	1.0013 (0.9998–1.0029)	1.0001 (0.9958–1.0044)
FHR	1.0134 (0.9801–1.0478)	1.1412 (0.9235–1.4103)	1.0226 (1.0020–1.0435)	1.0150 (0.9578–1.0756)
IL-6	0.9968 (0.9783–1.0156)	0.9941 (0.9717–1.1070)	1.0083 (1.0012–1.0154)	1.0079 (0.9998–1.0161)
sIL-2R	0.7885 (0.4441–1.3999)	0.6136 (0.2665–1.4130)	1.2440 (1.0251–1.5098)	1.1354 (0.8638–1.4923)

Abbreviations: CI, confidence interval; FHR, ferritin-hemoglobin ratio; IL-6, interleukin-6; OR, odds ratio; SE, standard error; sIL-2R, soluble interleukin-2 receptors.

and sIL-2R in patients aged ≥65 years may be used for prediction of severe/critical condition. Also, ferritin-hemoglobin ratio, IL-6, and sIL-2R in patients aged ≥65 years may be used for prediction of mortality according to unadjusted odds ratio. However, all tested biomarkers failed to show enough predictive abilities according to adjusted odds ratio.

DISCUSSION

Our study showed acceptable discriminative capabilities of ferritin, ferritin-hemoglobin ratio, sIL-2R for severe/critical condition. IL-6 failed to show sufficient discriminative capabilities for severe/critical condition. However, all these parameters had insufficient discriminative capabilities for lethal outcome. Among all participants, ferritin and ferritin-hemoglobin ratio showed sufficient predictive capabilities for severe/critical condition; the optimal cut-off criteria were 402.0 ng/mL and 34.0, respectively. Despite the fact that multiple studies have evaluated the discriminative and predictive capabilities of these biomarkers, impact of age on discriminative and predictive capabilities of COVID-19 severity and mortality has not been assessed.

There are controversial results of multiple studies regarding the discriminative and predictive capabilities of ferritin, IL-6, and sIL-2R for severe condition and mortality. Cao P. et al (2020) showed a high discriminative capability of ferritin for the severity of COVID-19 (AUC, 0.873) with an optimal cut-off value of 272.5 ng/mL (34). Also, the study performed by Deng F. et al (2021) showed a high discriminative capability for in-hospital mortality in COVID-19 patients treated in ICU (AUC, 0.822) (35). However, some studies showed far lower discriminative capability of ferritin for hospital mortality. Shakaroun D. A. et al. (2023) reported that ferritin for predicting hospital mortality had an AUC of 0.65 with a sensitivity of 65% and specificity of 58% at the optimal cut-off value (36). According to the FerVid study, the AUC of ferritin levels for adverse outcome prediction was 0.617 (21) which corresponds to our results. Some studies showed great variation in the discriminative capability of IL-6 for adverse outcomes. The study performed by Aykal G. et al (2021) showed a high AUC for IL-6 (0.864) (37). Jamoussi A. et al (2023) reported an AUC of 0.805 for ferritin level for mortality in COVID-19 patients managed in ICU (38). According to the study of Arnold D. T. et al (2021) IL-6 had an AUC of 0.77 (0.65–0.88) for the prediction of poor prognosis (39). However, Jang H. J. et al (2021) reported an AUC of 0.687 for the IL-6 level for in-hospital mortality in patients with respiratory failure, an optimal cut-off value of 191 pg/mL with a sensitivity of 50.0% and a specificity of 87.2% (29) that is similar to the results of our study. This study showed that an AUC for the predictive capability of sIL-2R for mortality was 0.718 (29). Such controversy may be explained by the fact that there were differences in studied populations and variability in the severity of COVID-19 at biomarker measurement.

Despite the evidence that levels of ferritin (28), IL-6 (40), and sIL-2R (32) increase with age, comparison of predictive abilities depending on the patients' age was not found. Our study showed the absence of discriminative capabilities of ferritin, ferritin-hemoglobin ratio, IL-6, and sIL-2R for severe/critical condition and lethal outcome in patients aged <65 years. Ferritin-hemoglobin ratio, IL-6, and sIL-2R had acceptable discriminative capabilities for severe/critical condition and lethal outcome in patients aged ≥65 years. Also, ferritin showed acceptable discriminative capabilities for severe/critical condition in patients aged ≥65 years. However, according to adjusted odds ratio, all studied biomarkers didn't show enough predictive abilities.

Further perspectives include the establishment of the influence of different age categories on discriminative and predictive capabilities of laboratory parameters on COVID-19 severity and mortality. Also, a study of other factors (gender, body mass index, comorbidities, etc.) on discriminative and predictive capabilities of laboratory parameters is a perspective.

CONCLUSIONS

Ferritin, ferritin-hemoglobin ratio, IL-6, and sIL-2R didn't show acceptable predictive value for severe condition and lethal outcome in patients aged <65 years. However, ferritin-hemoglobin ratio, IL-6, and sIL-2R have high predictive value for lethal outcome in patients aged ≥65 years. So, age may affect the predictive capabilities of these biomarkers.

REFERENCES

1. Kneip T, Börsch-Supan A, Andersen-Ranberg K. Social, health and economic impact of the COVID-19 pandemic from a European perspective. Eur J Ageing. 2022 Nov 14; 19(4): 789–92.
2. WHO. WHO COVID-19 dashboard (Internet). World Health Organization. 2023. Available from: https://covid19.who.int/ (Accessed 15-Oct-2023).
3. Our World in Data. Mortality Risk of COVID-19 – Statistics and Research (Internet). Our World in Data. Available from: https://ourworldindata.org/mortality-risk-covid (Accessed 15-Oct-2023).
4. Xie Y, Choi T, Al-Aly Z. Risk of Death in Patients Hospitalized for COVID-19 vs Seasonal Influenza in Fall-Winter 2022–2023. JAMA. 2023; 329(19): 1697–9.
5. Wang H, Paulson KR, Pease SA, Watson S, Comfort H, Zheng P. COVID-19 Excess Mortality Collaborators. Estimating excess mortality due to the COVID-19 pandemic: a systematic analysis of COVID-19-related mortality, 2020–21. Lancet. 2022 Apr 16; 399 (10334): 1513–36.
6. Tan LY, Komarasamy TV, Rmt Balasubramaniam V. Hyperinflammatory immune response and COVID-19: a double edged sword. Front Immunol. 2021; 12: 742941.
7. Khan A, Khan WM, Ayub M, Humayun M, Haroon M. Ferritin Is a Marker of Inflammation rather than Iron Deficiency in Overweight and Obese People. J Obes. 2016; 2016: 1937320.
8. DePalma RG, Hayes VW, O'Leary TJ. Optimal serum ferritin level range: iron status measure and inflammatory biomarker. Metallomics. 2021 Jun 11; 13(6): mfab030.
9. Kernan KF, Carcillo JA. Hyperferritinemia and inflammation. Int Immunol. 2017 Nov 1; 29(9): 401–9.
10. Zhou Z, Yang D, Li C, Wu T, Shi R. Serum ferritin and the risk of short-term mortality in critically ill patients with chronic heart failure: a retrospective cohort study. Front Physiol. 2023 Jul 13; 14: 1148891.
11. Ahmed S, Ansar Ahmed Z, Siddiqui I, Haroon Rashid N, Mansoor M, Jafri L. Evaluation of serum ferritin for prediction of severity and mortality in COVID-19 – A cross sectional study. Ann Med Surg (Lond). 2021 Mar; 63: 102163.
12. Kurian SJ, Mathews SP, Paul A, et al. Association of serum ferritin with severity and clinical outcome in COVID-19 patients: An observational study in a tertiary healthcare facility. Clin Epidemiol Glob Health. 2023 May–Jun; 21: 101295.
13. Mourji D, Abouelfath Z, Abassor T, et al. Association between Ferritin and COVID-19 Mortality in 1310 Moroccan Patients. Cross current international journal of medical and Biosciences. 2022 Jul 12; 4(3): 50–4.
14. Feld J, Tremblay D, Thibaud S, Kessler A, Naymagon L. Ferritin levels in patients with COVID-19: A poor predictor of mortality and hemophagocytic lymphohistiocytosis. Int J Lab Hematol. 2020 Dec; 42(6): 773–9.
15. Chicamy YA, Safitri A, Nindrea RD. Serum Ferritin Levels for the Prediction of Mortality among COVID-19 Patients in an Indonesia's National Referral Hospital. Open Access Maced J Med Sci. 2022 May 5; 10(B): 1056–61.
16. Raman N, Kv P, Ashta KK, Vardhan V, et al. Ferritin and Hemoglobin as Predictors of Fatal Outcome in COVID-19: Two Sides of the Same Coin. J Assoc Physicians India. 2021 Aug; 69(8): 11–12.
17. Aygun H, Eraybar S. Can ferritin/lymphocyte percentage ratio, a new indicator, predict the clinical course of COVID-19 cases? Bratisl Lek Listy. 2022; 123(6): 395–400.
18. Yurt NS, Ocak M. Ferritin/lymphocyte percentage ratio to predict the severity and mortality of COVID-19. Malawi Med J. 2023 Oct 11; 35(3): 183–9.
19. Taşkin Ö, Yilmaz A, Soylu VG, Demir U, Çatan IF. Ferritin/albumin ratio could be a new indicator of COVID-19 disease mortality. J Infect Dev Ctries. 2023 Jan 31; 17(1): 37–42.
20. Dahan S, Segal G, Katz I, et al. Ferritin as a Marker of Severity in COVID-19 Patients: A Fatal Correlation. Isr Med Assoc J. 2020 Aug; 22(8): 494–500.
21. Para O, Caruso L, Pestelli G, et al. Ferritin as prognostic marker in COVID-19: the FerVid study. Postgrad Med. 2022 Jan; 134(1): 58–63.
22. Anai M, Akaike K, Iwagoe H, et al. Decrease in hemoglobin level predicts increased risk for severe respiratory failure in COVID-19 patients with pneumonia. Respir Investig. 2021 Mar; 59(2): 187–93.
23. Xu Y, Yang H, Wang J, et al. Serum Albumin Levels are a Predictor of COVID-19 Patient Prognosis: Evidence from a Single Cohort in Chongqing, China. Int J Gen Med. 2021 Jun 24; 14: 2785–97.
24. Zerbato V, Sanson G, De Luca M, et al. The Impact of Serum Albumin Levels on COVID-19 Mortality. Infect Dis Rep. 2022 Apr 20; 14(3): 278–86.
25. Li Y, Yang T, Wang S, et al. The value of lymphocyte count in determining the severity of COVID-19 and estimating the time for nucleic acid test results to turn negative. Bosn J Basic Med Sci. 2021 Apr 1; 21(2): 235–41.
26. Ziadi A, Hachimi A, Admou B, et al. Lymphopenia in critically ill COVID-19 patients: A predictor factor of severity and mortality. Int J Lab Hematol. 2021 Feb; 43(1): e38–e40.
27. Liu J, Li H, Luo M, et al. Lymphopenia predicted illness severity and recovery in patients with COVID-19: A single-center, retrospective study. PLoS One. 2020 Nov 18; 15(11): e0241659.
28. Hadi JM, Mohammad HM, Ahmed AY, et al. Investigation of Serum Ferritin for the Prediction of COVID-19 Severity and Mortality: A Cross-Sectional Study. Cureus. 2022 Nov 28; 14(11): e31982.
29. Jang HJ, Leem AY, Chung KS, et al. Soluble IL-2R Levels Predict in-Hospital Mortality in COVID-19 Patients with Respiratory Failure. J Clin Med. 2021 Sep 18; 10(18): 4242.
30. Nikkhoo B, Mohammadi M, Hasani S, et al. Elevated interleukin (IL)-6 as a predictor of disease severity among Covid-19 patients: a prospective cohort study. BMC Infect Dis. 2023 May 9; 23(1): 311.
31. Luporini RL, Rodolpho JMA, Kubota LT, et al. IL-6 and IL-10 are associated with disease severity and higher comorbidity in adults with COVID-19. Cytokine. 2021 Jul; 143: 155507.
32. Motojima S, Hirata A, Fukuda T, Makino S. High serum soluble interleukin-2 receptor concentrations in elderly individuals and smokers. Arerugi. 1993 Nov; 42(11): 1715–20.
33. Ministerstvo Okhorony Zdorovia Ukrainy. Derzhavnyi Ekspertnyi Tsentr (Internet). Protokol "Nadannia medychnoi dopomohy dlia likuvannia koronavirusnoi khvoroby (COVID-19)" (cited 17-Oct-2023). Available from: https://www.dec.gov.ua/wp-content/uploads/2023/05/protokol-covid2023.pdf. Ukrainian.
34. Cao P, Wu Y, Wu S, et al. Elevated serum ferritin level effectively discriminates severity illness and liver injury of coronavirus disease 2019 pneumonia. Biomarkers. 2021 May; 26(3): 207–12.
35. Deng F, Zhang L, Lyu L, et al. Increased levels of ferritin on admission predicts intensive care unit mortality in patients with COVID-19. Med Clin (Engl Ed). 2021 Apr 9; 156(7): 324–31.
36. Shakaroun DA, Lazar MH, Horowitz JC, Jennings JH. Serum Ferritin as a Predictor of Outcomes in Hospitalized Patients with Covid-19 Pneumonia. J Intensive Care Med. 2023 Jan; 38(1): 21–6.
37. Aykal G, Esen H, Seyman D, Çalışkan T. Could IL-6 predict the clinical severity of COVID-19? Turk J Biochem. 2021 Oct 1; 46(5): 499–507.
38. Jamoussi A, Messaoud L, Jarraya F, et al. Interleukin-6 prediction of mortality in critically ill COVID19 patients: A prospective observational cohort study. PLoS One. 2023 Mar 1; 18(3): e0279935.
39. Arnold DT, Attwood M, Barratt S, et al. Predicting outcomes of COVID-19 from admission biomarkers: a prospective UK cohort study. Emerg Med J. 2021 Jul; 38(7): 543–8.
40. Wyczalkowska-Tomasik A, Czarkowska-Paczek B, Zielenkiewicz M, Paczek L. Inflammatory Markers Change with Age, but do not Fall Beyond Reported Normal Ranges. Arch Immunol Ther Exp (Warsz). 2016 Jun; 64(3): 249–54.

Atypical Manifestation of X-linked Agammaglobulinemia – the Importance of Genetic Testing

Adam Markocsy[1], Daniela Kapustová[1], Andrej Čereš[3], Eva Froňkova[4], Miloš Jeseňák[1,2,3,*]

ABSTRACT

X-linked agammaglobulinemia (XLA) was one of the first inborn errors of immunity to be described. It is caused by pathogenic variants in the gene for Bruton tyrosine kinase (BTK), which has important functions in B cell development and maturation. Recurrent bacterial infections in the first two years of life and hypogammaglobulinemia with absent B cells in male patients are the most common symptoms.
A four-month-old male patient underwent surgical removal of *urachus persistens* complicated with recurrent scar abscesses. Hypogammaglobulinemia (IgG, IgA, and IgM), low phagocytic activity, mild neutropenia, and a normal percentage of B cells were observed in the patient's immune laboratory profile. Over time, he suffered recurrent respiratory infections (otitis media and rhinosinusitis) and developed B cell depletion, but interestingly, this was with a normalisation of IgG and IgA levels along with undetectable IgM. Molecular-genetic testing confirmed the presence of the pathogenic variant c.1843C>T in the BTK gene, which is associated with a milder phenotype of XLA.
Molecular-genetic testing uncovers the variability of clinical and laboratory features of apparently well-known inherited disorders. Patients with mild "leaky" XLA may have normal levels of non-functional or oligoclonal immunoglobulins.

KEYWORDS

atypical leaky phenotype; Inborn error of immunity; X-linked agammaglobulinemia; molecular-genetic testing; BTK gene

AUTHOR AFFILIATIONS

[1] Centre for Primary Immunodeficiencies, Department of Paediatrics, Jessenius Faculty of Medicine, Comenius University in Bratislava, University Hospital in Martin, Slovakia
[2] Centre for Primary Immunodeficiencies, Department of Pulmonology and Phthisiology, Jessenius Faculty of Medicine, Comenius University in Bratislava, University Hospital in Martin, Slovakia
[3] Department of Clinical Immunology and Allergology, Jessenius Faculty of Medicine, Comenius University in Bratislava, University Hospital in Martin, Slovakia
[4] CLIP Laboratory Centre, Department of Paediatric Haematology and Oncology, Second Faculty of Medicine, Charles University and University Hospital Motol, Prague, Czech Republic
* Corresponding author: Jessenius Faculty of Medicine of Comenius University in Bratislava, Kollárova 2, 036 59 Martin, Slovak Republic; e-mail: jesenak@gmail.com

Received: 9 June 2024
Accepted: 7 August 2024
Published online: 22 October 2024

Acta Medica (Hradec Králové) 2024; 67(2): 60–63
https://doi.org/10.14712/18059694.2024.21

INTRODUCTION

X-linked agammaglobulinemia (XLA) is a long-known inborn error of immunity (IEI) that was first described by paediatrician Ogden Bruton in 1952 (1). Affected male patients typically present with recurrent bacterial infections; hypogammaglobulinemia; rudimentary adenoidal, tonsillar tissue; peripheral lymphoid hypoplasia; and an absence of mature B cells in peripheral blood. Typical identified pathogens are the encapsulated bacteria *Streptococcus pneumoniae*, *Haemophilus influenzae*, and *Neisseria meningitidis*, but patients also suffer from giardiasis (lambliasis) and meningoencephalitis caused by echoviruses (2). In addition, autoimmune and inflammatory complications have been reported, but only rarely (3). Clinical diagnostic criteria established by the European Society for Immunodeficiencies (ESID) are shown in Table 1 (4). XLA is caused by pathogenic loss of function variants in the gene for BTK, which has an essential function in B cell development and maturation in the bone marrow. The most profound defect is in development from the pre-B cell stage to the immature B cell stage; maturation of pro-B cells and immature B cells is also defective in this condition (5). BTK expression is primarily restricted to hematopoietic cells – B cells, monocytes, myeloid cells, erythrocyte precursors, and megakaryocytes. In XLA patients, only a decrease in B cells has been observed, suggesting that BTK may be redundant for the maturation of other cell types (5). Immunoglobulin replacement and antibiotic prophylaxis is used in XLA therapy. In selected, very severe cases, hematopoietic stem cell transplantation is another treatment option (6). In rare cases, females can also develop symptoms due to skewed (non-random) inactivation of the non-mutated X-chromosome in hematopoietic cells (7, 8).

More pathogenic variants associated with a milder course of disease have been reported in the literature (9–11); they lead to decreased BTK expression but not to a total absence of BTK expression or the production of a partially functional mutated protein. This condition is referred to as leaky or mild XLA – the patients become symptomatic with typical associated-infection complications but at an older age. Patients with leaky XLA can have higher proportion of B cells as in typical XLA (more than 2%) and only slightly decreased to normal immunoglobulin values. Patients with mild XLA can be misdiagnosed with common variable immunodeficiency (11). There is no definite correlation between the type of variant (missense, nonsense, etc.) in the BTK gene and the severity of the disease (12).

Tab. 1 Clinical diagnostic criteria for X-linked agammaglobulinemia.

Definitive diagnosis
Male patient with < 2% CD19⁺ B cells and at least one of the following:
1. Mutation in BTK gene 2. Absent BTK mRNA on northern blot analysis of neutrophils or monocytes 3. Absent BTK protein in monocytes or platelets 4. Maternal cousins, uncles or nephews with less than 2% CD19⁺ B cells
Probable diagnosis
Male patient with < 2% CD19⁺ B cells in whom:
Other causes of hypogammaglobulinemia have been excluded and all of the following: 1. Onset of recurrent bacterial infections in the first 5 years of life 2. Serum IgG, IgM and IgA more than 2SD below normal for age 3. Absent isohemagglutinins and /or poor response to vaccines
Possible diagnosis
Male patient with < 2% CD19⁺ B cells in whom:
Other causes of hypogammaglobulinemia have been excluded and at least one of the following: 1. Onset of recurrent bacterial infections in the first 5 years of life 2. Serum IgG, IgM and IgA more than 2SD below normal for age 3. Absent isohemagglutinins and /or poor response to vaccines

Legend: SD – standard deviation.

CASE REPORT

At the age of four months, a male patient born after an uneventful first pregnancy and with normal postnatal adaptation underwent a surgical removal of *urachus persistens* that was complicated by recurrent scar abscesses (three times), a C-reactive protein level of 208 mg/L (reference range: 0–5 mg/L), and poor healing. Cultures of from the abscess fluid were repeatedly positive for *Staphylococcus aureus*. Hypogammaglobulinemia, low phagocytic activity (50%, reference range: 80–100%), low phagocytic index (4, reference range: >30), and mild neutropenia were observed in the patient's laboratory parameters. Flow cytometry showed no significant deviations; the patient's percentage of B cells was normal but with a significant decrease in the proportion of switched memory B cells. Selected laboratory parameters are shown in Table 2.

Over time, the patient suffered recurrent respiratory infections, recurrent otitis media with positive cultivation of *Streptococcus pneumoniae*, and mouth ulcers. He underwent *Salmonella* gastroenteritis and SARS-CoV2 infection with mild respiratory symptoms, and he was diagnosed with allergic rhinitis caused by grass allergy. After the solving of abscess complications, the patient's phagocytic activity, phagocytic index, and neutropenia normalised. He developed B cell depletion in blood, but, interestingly, this was accompanied by the normalisation of IgG and IgA levels and a persisting depletion of IgM. Flow cytometry showed an elevation of transitional B cells, $CD21^{low}$ B cells, and a normal proportion of marginal zone cells such as B cells, switched memory B cells, naïve B cells, and double-negative T cells. Mild IgG_1 subclass deficiency (3,27 g/L, reference range: 3.80–9.30 g/L) was identified at 8 years of age, but other IgG subclasses had normal values. Diagnostic vaccination was not performed because of parents' refusal. The patient had a negative family history for IEI-associated complications or monogenic disorders. Molecular-genetic testing was performed (massive parallel sequencing focusing on a panel for primary immunodeficiencies) because of recurrent infections and significant B cell depletion, which confirmed the presence of the

Tab. 2 Changes of laboratory parameters over time.

Age	4 months	7 months	16 months	4 years	6 years	8 years	10 years
IgG [g/l]	**1.59**	**1.12**	**3.27**	6.11	6.57	6.17	6.58
IgA [g/l]	**0.05**	**0.05**	**0.07**	0.84	0.86	1.17	1.43
IgM [g/l]	**0.05**	**0.24**	**0.14**	**0.29**	**0.06**	**0.05**	**0.12**
IgE [IU/l]	25.00	46.00	27.70	51.70	56.90	24.00	48.90
leukocytes [x 10^9/l]	6.60	11.30	7.50	7.90	6.70	5.50	4.60
neutrophils [x 10^9/l]	**1.20**	3.90	2.20	4.20	1.30	2.80	2.90
lymphocytes [x 10^9/l]	4.70	5.80	4.20	2.90	2.26	2.12	2.70
$CD3^+$ T cells [%]	**84.00**	80.00	**82.00**	**90.00**	**81.00**	**90.00**	79.00
$CD3^+$ T cells [x 10^9/l]	**4.03**	**4.66**	**3.38**	**2.64**	1.82	1.91	1.64
$CD19^+$ B cells [%]	10.00	12.00	**3.00**	**1.00**	**3.00**	**1.00**	**2.00**
$CD19^+$ B cells [x 10^9/l]	0.25	0.72	**0.11**	**0.022**	**0.064**	**0.021**	**0.041**
transitional B cells [%]					**27.80**	**32.00**	**32.50**
switched memory B cells [%]					**2.10**	11.00	13.60
$CD21^{low}$ B cells [%]					**9.10**	**22.70**	5.00

Legend: Values below reference range specific for age are marked with bold writing in blue color, values above reference range specific for age are marked with bold writing in red color. Mild neutropenia: 1.0–1.5 × 10^9/l of neutrophils in blood. All laboratory parameters were collected during the stable course of disease without ongoing infection complications. We did not perform B cell phenotypic profiling until 6 years of age because of technical limitations of flow cytometry analysis in our laboratory.

pathogenic c.1843C>T, p.Arg615Cys missense variant in the BTK gene (NM_000061.3).

The identified missense variant is located in the kinase domain of the gene that is responsible for the catalytic activity of BTK; it is considered pathogenic according to ACMG criteria (PS3, PM1, PM2, PM5, PP3). The variant was evaluated twice as a variant of uncertain significance in the ClinVar database. In silico prediction tools classify this variant either pathogenic, pathogenic supporting, or uncertain. The CADD score for this variant is high with a value of 32, its population frequency is very low (0.000000913 in gnomAD), and its conservation score is high (10.003 in PhyloP100way). The variant has previously been described by Kraft et al. in a 34-year-old male patient with recurrent infections, hypogammaglobulinemia, a decreased percentage of B cells (2.9%), and decreased BTK protein expression as determined by flow cytometry in $CD20^+$ B cells and $CD14^+$ monocytes (13). Alternative variants at the same amino acid position (p.Arg615Ser, p.Arg615Pro) were described in XLA patients, both in a male patient with a mild course of disease and IgG hypogammaglobulinemia (1,8 g/L), and in another male patient with decreased *BTK* expression (12, 14).

DISCUSSION

A male patient with recurrent respiratory infections, otitis media, scar abscesses, and the significant depletion of B cells was genetically diagnosed with XLA. Interestingly, the patient did not have this B cell depletion at the age of 4 months, and IgG and IgA levels normalised over time. A missense variant c.1843C>T in the BTK gene met the genotype–phenotype correlation in our patient, and we consider it causal for mild "leaky" XLA.

As we did not perform B cell phenotypic profiling at the beginning of follow up, we cannot say which B cell developmental stage was responsible for the normal B cell proportion, but we later saw the elevation of transitional B cells that represent a developmental stage between immature B cells in the bone marrow and mature peripheral B cells. The BTK gene is also important in the development of immature B cells, which could be the explanation for this observation. The identified pathogenic variant was not associated with a total absence of BTK expression, but only with its decrease, so we expect that a small proportion of pre-B cells has been able develop to stages capable of immunoglobulin production. The observed proportion of switched memory B cells is probably responsible for the increased production of endogenous immunoglobulins between 2 and 4 years of age. A small number of leaked mature B cells had possibly been distributed in local lymphoid tissues, such as bone marrow or lymph node; the produced immunoglobulins were non-functional or oligoclonal and therefore less effective than immunoglobulins produced by B cells of the healthy individual. There is an indication for immunoglobulin replacement therapy in case of recurrent infections.

CONCLUSIONS

Patients with leaky XLA may have normal levels of non-functional or oligoclonal immunoglobulins, and there is the indication for immunoglobulin replacement therapy in case of recurrent infections. Molecular-genetic testing uncovers the variability of clinical and laboratory features of apparently well-known inherited disorders. We should therefore consider molecular-genetic testing in IEI patients with atypical presentation or mild symptoms.

ACKNOWLEDGMENTS

This publication has been produced with the support of the Integrated Infrastructure Operational Program for the following project: Systemic Public Research Infrastructure – Biobank for Cancer and Rare Diseases, ITMS: 313011AFG5, which was co-financed by the European Regional Development Fund.

REFERENCES

1. Bruton OC. Agammaglobulinemia. Pediatrics. 1952; 9(6): 722–8.
2. Havlicekova Z, Jesenak M, Freiberger T, Banovcin P. X-linked agammaglobulinemia caused by new mutation in BTK gene: A case report. Biomed Pap Med Fac Univ Palacky Olomouc Czech Repub. 2014; 158(3): 470–3.
3. Hernandez-Trujillo VP, Scalchunes C, Cunningham-Rundles C, et al. Autoimmunity and inflammation in X-linked agammaglobulinemia. J Clin Immunol. 2014; 34(6): 627–32.
4. European Society for Immunodeficiencies. X-Linked Agammaglobulinemia. (Accessed May 15, 2024), at https://esid.org/Education/X-Linked-Agammaglobulinemia.
5. Gaspar HB, Kinnon C. X-linked agammaglobulinemia. Immunol Allergy Clin North Am. 2001; 21(1): 23–43.
6. Nishimura A, Uppuluri R, Raj R, et al. An International Survey of Allogeneic Hematopoietic Cell Transplantation for X-Linked Agammaglobulinemia. J Clin Immunol. 2023; 43(8): 1827–39.
7. Takada H, Kanegane H, Nomura A, et al. Female agammaglobulinemia due to the Bruton tyrosine kinase deficiency caused by extremely skewed X-chromosome inactivation. Blood. 2004; 103(1): 185–7.
8. Vysehradska J, Strakova J, Fedor M, Vysehradsky R, Banovcin P. Hypogamaglobulinaemia with complete absence of B-lymphocytes in a 16-year-old patient. Pediatria (Bratisl.). 2006; 1(3): 168–71.
9. Kornfeld SJ, Good RA, Litman GW. Atypical X-linked agammaglobulinemia. N Engl J Med. 1994; 331: 949–51.
10. Usui K, Sasahara Y, Tazawa R, et al. Recurrent pneumonia with mild hypogammaglobulinemia diagnosed as X-linked agammaglobulinemia in adults. Respir Res. 2001; 2(3): 188–92.
11. Sigmon JR, Kasasbeh E, Krishnaswamy G. X-linked agammaglobulinemia diagnosed late in life: case report and review of the literature. Clin Mol Allergy. 2008; 6: 5.
12. Kanegane H, Futatani T, Wang Y, et al. Clinical and mutational characteristics of X-linked agammaglobulinemia and its carrier identified by flow cytometric assessment combined with genetic analysis. J Allergy Clin Immunol. 2001; 108(6): 1012–20.
13. Kraft MT, Pyle R, Dong X, et al. Identification of 22 novel BTK gene variants in B cell deficiency with hypogammaglobulinemia. Clin Immunol. 2021; 229: 108788.
14. Abolhassani H, Vitali M, Lougaris V, et al. Cohort of Iranian Patients with Congenital Agammaglobulinemia: Mutation Analysis and Novel Gene Defects. Expert Rev Clin Immunol. 2016; 12(4): 479–86.

VIPoma: An Unusual Cause of Chronic Diarrhea

Sutharin Suteetorn[1,2], Krit Kitisin[3], Natcha Wanpiyarat[4], Supaksorn Kunjan[5], Thiti Snabboon[2,6,*]

ABSTRACT

Chronic diarrhea is a significant challenge in clinical practice because of its high prevalence and various causes. Comprehensive clinical assessment and stepwise laboratory approach are crucial for an accurate diagnosis. This report presents a case of an adult woman who experienced chronic watery diarrhea, complicated by renal impairment and multiple electrolyte imbalances, including hypokalemia, hypophosphatemia, and metabolic acidosis. The diagnosis of a vasoactive intestinal polypeptide-secreting tumor (VIPoma) with liver metastases was confirmed by elevated serum levels of a vasoactive intestinal polypeptide (VIP) and imaging findings of a pancreatic mass with multiple hepatic lesions. Preoperative management, including fluid rehydration, electrolyte correction, and somatostatin analog therapy, significantly improved her clinical symptoms. Subsequent surgical tumor removal and radiofrequency ablation of the hepatic lesions resulted in complete resolution of symptoms and normalized VIP levels. This case emphasizes the importance of early recognition of this rare tumor in patients with chronic diarrhea to improve clinical outcomes.

KEYWORDS

VIPoma; vasoactive intestinal polypeptide; WDHA syndrome; functional neuroendocrine tumor; chronic watery diarrhea

AUTHOR AFFILIATIONS

[1] Department of Medicine, Queen Savang Vadhana Memorial Hospital, Chonburi province, Thailand
[2] Department of Medicine, Faculty of Medicine, Chulalongkorn University, Bangkok, Thailand
[3] Department of Surgery, Faculty of Medicine, Chulalongkorn University, Bangkok, Thailand
[4] Department of Pathology, Faculty of Medicine, Chulalongkorn University, Bangkok, Thailand
[5] Center for Medical Diagnostic Laboratories, Faculty of Medicine, Chulalongkorn University, Bangkok, Thailand
[6] Excellence Center in Diabetes, Hormone and Metabolism, King Chulalongkorn Memorial Hospital, Thai Red Cross Society, Bangkok, Thailand
* Corresponding author: Excellence Center in Diabetes, Hormone and Metabolism, BhumiSirimangalanusorn Bldg., 4C fl, King Chulalongkorn Memorial Hospital, Thai Red Cross Society, Chulalongkorn University, Rama IV Road, Pathumwan, Bangkok, Thailand, 10330; e-mail: Thiti.S@chula.ac.th

Received: 3 June 2024
Accepted: 24 August 2024
Published online: 22 October 2024

Acta Medica (Hradec Králové) 2024; 67(2): 64–68
https://doi.org/10.14712/18059694.2024.22

INTRODUCTION

Chronic diarrhea is defined as loose or watery stools (Bristol Stool Chart types 5 to 7) that occur more than three times a day for at least four weeks (1). Its etiologies have a wide spectrum, including infectious diseases, inflammatory bowel diseases, malabsorption disorders, irritable bowel syndrome, food allergies, and adverse drug reactions. Endocrine disorders, such as thyrotoxicosis, hypoparathyroidism, Addison's disease, and diabetes mellitus, as well as functioning endocrine tumors, can also contribute to this clinical entity. This report presents a case of an adult female patient with chronic and severe diarrhea, subsequently diagnosed with a vasoactive intestinal polypeptide-secreting tumor (VIPoma). The diagnostic approach and treatment of this tumor have also been discussed.

CASE REPORT

A 62-year-old Thai woman presented with a one-year history of progressively worsening watery diarrhea. Her medical history included well-controlled type 2 diabetes, hypertension, and dyslipidemia diagnosed six years before. Initially, her diarrhea was treated as gastroenteritis with oral antibiotics at a local hospital. However, she continued to experience recurrent episodes of non-bloody, watery diarrhea exceeding 500–600 mL, with a frequency of more than 10 times daily. These episodes were unrelated to meals or food types and did not respond to loperamide.

The patient reported debilitating fatigue and significant weight loss of 12 kg. She denied fever, recent travel, laxative abuse, or illicit drug use. Physical examination revealed dehydration, cachexia, and proximal muscle weakness. Her vital signs were remarkable for tachycardia (105–110 bpm) and low blood pressure (80–90/50–60 mmHg). Laboratory tests showed renal insufficiency (creatinine 2.12 mg/dL), hyponatremia (134 mEq/L), severe hypokalemia (2.2 mEq/L), hypophosphatemia (1.8 mg/dL), and metabolic acidosis (bicarbonate 8 mEq/L). An electrocardiogram revealed sinus tachycardia with a prolonged QTc interval. Multiple stool examinations were negative for occult blood, parasites, and bacterial infections, including *Clostridium difficile*. Gastrointestinal endoscopy findings were unremarkable. Supportive treatment with intravascular fluids, parenteral nutrition, sodium bicarbonate, and potassium replacement was promptly initiated. The diagnosis of VIPoma was confirmed by significantly elevated serum vasoactive intestinal peptide (VIP) levels of 328 pg/mL (reference range: <75 pg/mL) and plasma chromogranin A (CgA) levels of 161.76 ng/mL (reference range: 27–94 ng/mL). Other laboratory findings included urine 5-HIAA levels of 4.48 mg/24 hours (reference range: 2–8 mg/24 hours) and serum gastrin levels of 32 pg/mL (reference range: 13–115 pg/mL). Computed tomography (CT) revealed a large, well-circumscribed, lobulated, heterogeneously enhancing mass in the body and tail of the pancreas. Additionally, multiple well-defined enhancing lesions were identified in the liver, highly suggestive of hepatic metastasis (Figure 1). A short-acting somatostatin

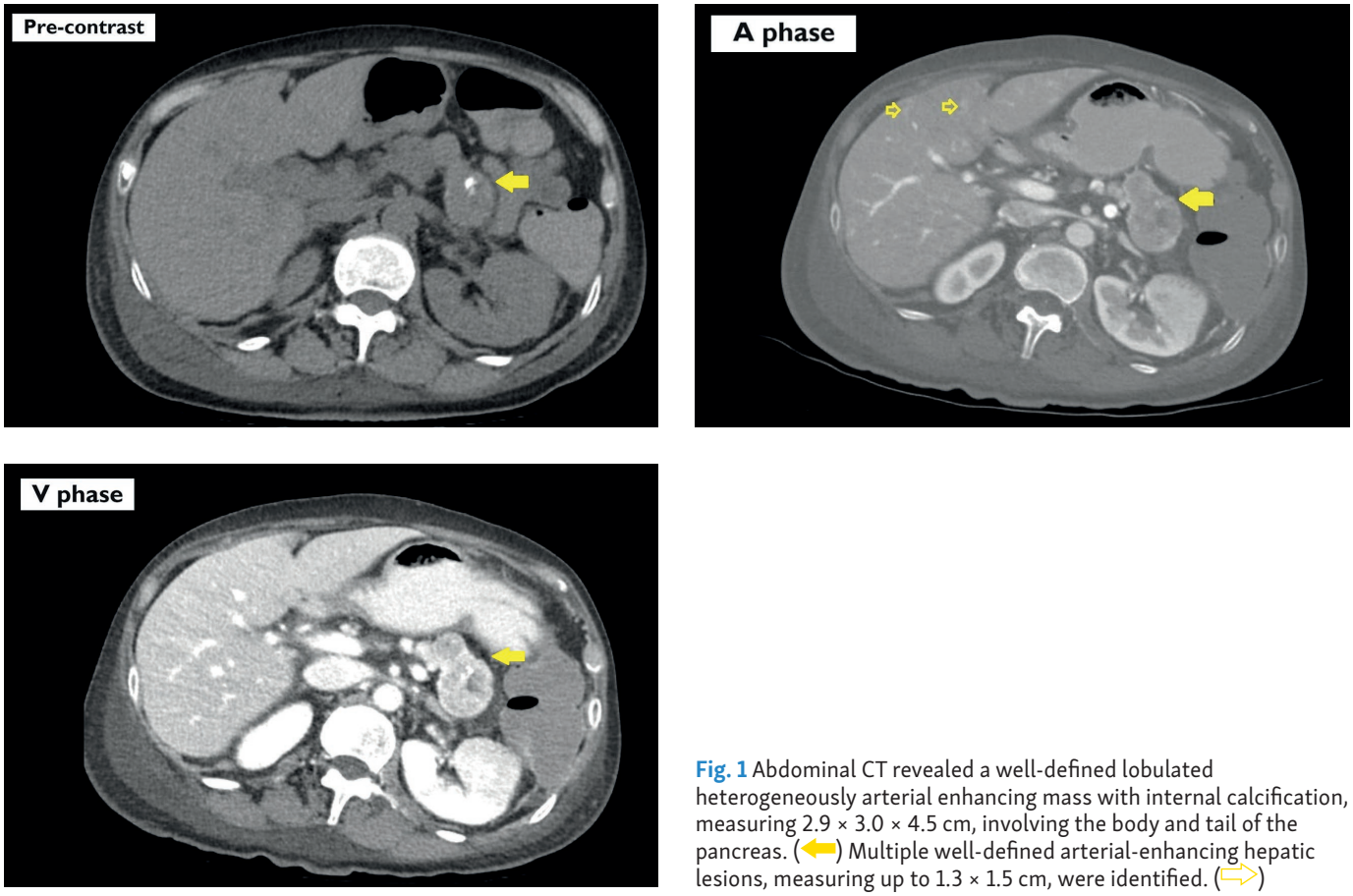

Fig. 1 Abdominal CT revealed a well-defined lobulated heterogeneously arterial enhancing mass with internal calcification, measuring 2.9 × 3.0 × 4.5 cm, involving the body and tail of the pancreas. (⬅) Multiple well-defined arterial-enhancing hepatic lesions, measuring up to 1.3 × 1.5 cm, were identified. (⇨)

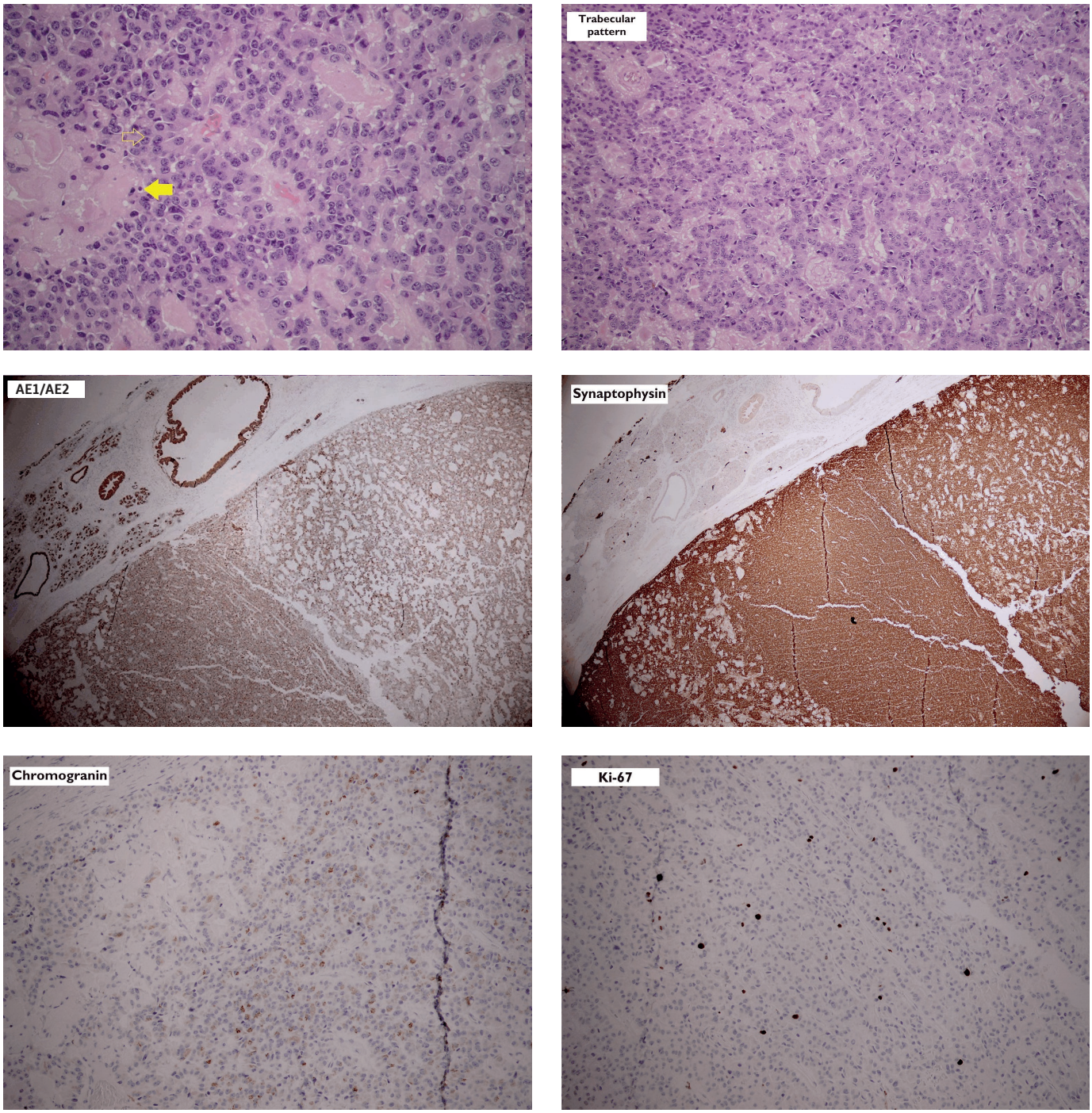

Fig. 2 Histopathology revealed epithelioid-shaped cells with uniform nuclei (⇨), arranged in a trabecular pattern in a hyalinized background. (⬅) Immunohistochemically, the tumor cells showed diffuse reactivity with synaptophysin and AE1/AE3 (cytoplasmic staining), while only a small portion of tumor cells exhibited reactivity with chromogranin A. The Ki-67 index was 5%.

analog (SSA), octreotide, was initiated at a dose of 50 mg subcutaneously every 12 hours and increased to 250 mg every 6 hours as symptoms improved. Distal pancreatectomy, splenectomy, cholecystectomy, and wedge liver resection with intraoperative radiofrequency ablation were performed with successful outcomes. Pathological examination revealed a well-differentiated grade 2 neuroendocrine tumor according to the European Neuroendocrine Tumor Society (ENETS) criteria. Immunohistochemical staining demonstrated diffuse positivity for synaptophysin and AE1/AE3 and focal positivity for CgA (Figure 2). Lymphovascular and perineural invasions were identified. The mitotic rate was low (1 per 2 mm²) and the Ki-67 proliferation index was 5%. Based on the American Joint Committee on Cancer (AJCC) Eighth Edition criteria, the tumor was classified as stage IV (T4, N1, M1). Postoperatively, the patient achieved clinical recovery and did not require further SSA therapy. Throughout the 12-month follow-up period, functional imaging and serological studies showed no evidence of disease recurrence. Genetic testing for multiple endocrine neoplasia type 1 (MEN1) syndrome was negative.

DISCUSSION

This report describes a case of VIPoma, a rare etiology of chronic diarrhea. Despite our patient having distinct symptoms of this tumor, there was a delay in diagnosis, resulting in an advanced stage at presentation and an increased risk of life-threatening complications.

Chronic diarrhea can be categorized into four main types: watery, malabsorptive, inflammatory, and functional (1). Watery diarrhea can be further classified into osmotic or secretory types through fasting trials. The diagnostic process involves a detailed history, a thorough physical examination, and appropriate investigations. It is also important to review medication history and screen for irritable bowel syndrome. Based on the stool characteristics and persistent symptoms during fasting in our patient, a secretory diarrhea subtype was suspected despite the unavailability of stool osmotic gap testing at our facility. Following a comprehensive workup to exclude common etiologies, including stool examinations, gastrointestinal endoscopy, and evaluation for prevalent endocrine disorders, we investigated less frequent hormone-secreting neuroendocrine tumors, such as carcinoid, gastrinoma, and VIPoma.

VIPoma is an extremely rare functional neuroendocrine neoplasm, accounting for less than 5% of all pancreatic neuroendocrine tumors, with an estimated annual incidence of 1 per 10 million individuals (2). The tumor is described in various terms, including pancreatic cholera, WDHA (watery diarrhea, hypokalemia, achlorhydria), and Verner-Morrison syndrome. Most affected individuals are adults between the ages of 30 and 50, with a slight female predominance (3). About 90% of these tumors are in the body and tail of the pancreas, while the remaining originate in extra-pancreatic tissues such as the adrenal medulla or sympathetic ganglia, particularly in pediatric patients (4). These tumors usually present as solitary lesions, often larger than 3 cm in size, and approximately 80% have metastasized at the time of diagnosis, primarily to the liver (5). Most cases of VIPoma occur sporadically, with about 5% of cases associated with MEN1 syndrome (6).

VIP, a neuropeptide, has significant effects on various physiological processes, including the regulation of pancreatic enzyme and gastric acid secretion, vasodilation, and intestinal motility. These effects are mediated through the activation of cyclic adenosine monophosphate (cAMP) and adenylate cyclase. Patients with VIPoma typically experience chronic and profuse secretory diarrhea, with stool volume exceeding 3 liters per day. Notably, the stool is odorless, tea-colored, and free of blood or mucus. VIP-mediated potassium secretion from intestinal cells leads to hypokalemia, while concurrent bicarbonate wasting contributes to metabolic acidosis. Its inhibitory effect on gastric parietal cells resulting in hypo- or achlorhydria leads to malabsorption. Co-secretion with other islet cell peptides, such as gastrin and pancreatic polypeptide, is observed in approximately 30–50% of cases (7). Severe dehydration can lead to renal failure and hypercalcemia. In patients with MEN1 syndrome, hypercalcemia may be attributed to concurrent hyperparathyroidism. Additionally, VIP has a glycogenolytic effect on the liver, contributing to hyperglycemia in up to 50% of cases. Other less common symptoms, including flushing, bloating, nausea, vomiting, and weight loss, have been described (8).

The diagnosis of VIPoma is based on elevated serum VIP levels, with levels above 75 pg/mL considered indicative and values exceeding 200 pg/mL strongly suggestive (9). However, these levels can fluctuate between episodes of diarrhea. Due to the rarity of the tumor, nonspecific symptoms, and limited availability of diagnostic tools, the definitive diagnosis often takes over a year from symptom onset, as observed in our patient. Both CT and magnetic resonance imaging (MRI) have sensitivities of 75–100% in identifying tumors. While transabdominal ultrasonography (USG) has a lower sensitivity of 60%, it can serve as an initial imaging modality to guide further diagnostic investigations (10). Additionally, endoscopic ultrasound (EUS) provides higher-resolution images and enables fine-needle aspiration of tumors. Functional imaging techniques, such as somatostatin receptor scintigraphy or Ga-68 DOTATATE Positron Emission Tomography-Computed Tomography (PET-CT), have emerged as valuable methods for detecting metastatic lesions because of their high expression of somatostatin receptors.

Surgical resection is the main treatment for both primary and metastatic lesions, effectively improving symptoms and extending disease-free intervals. Preoperative care is crucial to ensure adequate hydration, appropriate blood glucose control, phosphate replacement, and correction of electrolyte abnormalities. SSA is the cornerstone of medical therapy, effectively controlling diarrhea up to 65% (10). This medication can decrease VIP levels and potentially stabilize tumor growth. In cases of resistance or tachyphylaxis to SSA, glucocorticoids, loperamide, and opiates may be added (11). Other interventions, such as systemic chemotherapy, interferon, radiofrequency ablation, and embolization, have yielded varying successes in treating unresectable or metastatic lesions. Molecular targeted drugs, such as sunitinib and everolimus, as well as peptide receptor radionuclide therapy (PRRT) using 177Lu-DOTATATE, have emerged as promising options (12). The prognosis is excellent for patients who undergo successful surgical removal of benign tumors without distant metastases, with 5-year survival rates reported exceeding 90%. Conversely, patients with distant metastases have a significantly lower estimated 5-year survival rate of around 60% (13).

CONCLUSION

This case report describes a rare tumor, VIPoma, which presents a significant clinical challenge in terms of diagnosis and management. Clinicians should consider this tumor in patients with chronic diarrhea that remains undiagnosed. Preoperative treatment with SSA administration followed by definitive surgical removal plays a crucial role in achieving successful outcomes. Furthermore, multidisciplinary management may improve the prognosis, even in advanced-stage patients.

REFERENCES

1. Arasaradnam RP, Brown S, Forbes A, et al. Guidelines for the investigation of chronic diarrhoea in adults: British Society of Gastroenterology, 3rd edition. Gut. 2018; 67(8): 1380–99.
2. Anderson CW, Bennett JJ. Clinical Presentation and Diagnosis of Pancreatic Neuroendocrine Tumors. Surg Oncol Clin N Am. 2016; 25(2): 363–74.
3. Jensen RT, Cadiot G, Brandi ML, et al. Consensus Conference participants. ENETS Consensus Guidelines for the management of patients with digestive neuroendocrine neoplasms: functional pancreatic endocrine tumor syndromes. Neuroendocrinology. 2012; 95(2): 98–119.
4. Belei OA, Heredea ER, Boeriu E, et al. Verner-Morrison syndrome. Literature review. Rom J Morphol Embryol. 2017; 58(2): 371–6.
5. Schizas D, Mastoraki A, Bagias G, et al. Clinicopathological data and treatment modalities for pancreatic vipomas: a systematic review. J BUON. 2019; 24(2): 415–23.
6. Chen C, Zheng Z, Li B, et al. Pancreatic VIPomas from China: Case reports and literature review. Pancreatology. 2019; 19(1): 44–9.
7. Yao JC, Eisner MP, Leary C, et al. Population based study of islet cell carcinoma. Ann Surg Oncol. 2007; 14(12): 3492–500.
8. Ghaferi AA, Chojnacki KA, Long WD, Cameron JL, Yeo CJ. Pancreatic VIPomas: subject review and one institutional experience. J Gastrointest Surg. 2008; 12(2): 382–93.
9. De Herder WW. Biochemistry of neuroendocrine tumours. Best Pract Res Clin Endocrinol Metab. 2007; 21(1): 33–41.
10. Pavel M, Öberg K, Falconi M, et al. Gastroenteropancreatic neuroendocrine neoplasms: ESMO Clinical Practice Guidelines for diagnosis, treatment and follow-up. Ann Oncol. 2020; 31(7): 844–60.
11. Azizian A, König A, Ghadimi M. Treatment options of metastatic and nonmetastatic VIPoma: a review. Langenbecks Arch Surg. 2022; 407(7): 2629–36.
12. Halfdanarson TR, Strosberg JR, Tang L, et al. The North American Neuroendocrine Tumor Society Consensus Guidelines for Surveillance and Medical Management of Pancreatic Neuroendocrine Tumors. Pancreas. 2020; 49(7): 863–81.
13. Smith SL, Branton SA, Avino AJ, et al. Vasoactive intestinal polypeptide secreting islet cell tumors: a 15-year experience and review of the literature. Surgery. 1998; 124(6): 1050–5.

Delayed-Onset Muscle Soreness of the Psoas Major Muscle Following Abdominal Training: Case Report

Laura Gabriela Silva[1], Victor Sudário Takahashi[2], José Luiz Masson de Almeida Prado[3], Henrique Shimidu[4], Luís Henrique Paiva D'Elia[5], Márcio Luís Duarte[2,6,*]

ABSTRACT

Edema of the psoas major muscle can indicate various pathologies, such as infection, malignancy, and trauma, but it can also result from benign causes like delayed-onset muscle soreness (DOMS). This article presents the case of a 44-year-old female patient who developed DOMS in the psoas major after participating in an intense abdominal workout. The patient reported hip pain that began a day after the workout, which was confirmed by magnetic resonance imaging (MRI) revealing significant edema in the psoas major muscles, particularly on the right side. Conservative treatment with rest and analgesics led to full recovery within two weeks. DOMS, typically associated with eccentric exercises, can be mistaken for more serious conditions, but its recognition is crucial to avoid unnecessary investigations and interventions. This case highlights the importance of clinical history and imaging findings in distinguishing DOMS from other causes of muscle edema, emphasizing the need for accurate diagnosis to ensure appropriate management.

KEYWORDS

magnetic resonance imaging; psoas muscles; delayed-onset muscle soreness

AUTHOR AFFILIATIONS

[1] Centro Universitário Atenas, Paracatu-MG, Brazil
[2] Universidade de Ribeirão Preto Campus Guarujá, Guarujá-SP, Brazil
[3] Fleury Medicina e Saúde, São Paulo-SP, Brazil
[4] Hospital Samaritano, São Paulo-SP, Brazil
[5] Live Core Funcional, Santos-SP, Brazil
[6] Diagnósticos da América S.A. – DASA, São Paulo-SP, Brazil
* Corresponding author: Universidade de Ribeirão Preto Campus Guarujá. Avenida Dom Pedro I, 3300 Guarujá-SP, Brazil. ZIP CODE: 11440-003; e-mail: marcioluisduarte@gmail.com

Received: 13 April 2024
Accepted: 26 August 2024
Published online: 22 October 2024

Acta Medica (Hradec Králové) 2024; 67(2): 69–71
https://doi.org/10.14712/18059694.2024.23

INTRODUCTION

The psoas major is a muscle attached to the T12-L4 vertebral bodies and the L1-L5 transverse processes at its origin. Its primary function is hip flexion, but it also contributes to lateral flexion of the spine (1). Edema of the psoas muscle is a non-specific finding that, while not commonly observed, can indicate a variety of conditions. One of the primary causes of psoitis is infection, which can occur either directly due to pathogens like *Staphylococcus aureus* or other Gram-negative bacteria, often following injections or injuries, especially in immunocompromised patients. Psoitis can also arise secondarily from the spread of infections from other organs, such as kidney abscesses, gastrointestinal inflammatory diseases, osteomyelitis, and other conditions (2). Trauma or injury can also cause isolated swelling or inflammation of the psoas muscles. In elderly individuals, spontaneous tendon tears can occur even without prior injury, leading to high signal intensity in the iliopsoas muscle near the injury site (3).

Edema in the psoas muscle can also result from malignancy, whether from a primary tumor or metastasis. However, one of the rarer causes of such edema is focal myositis, a benign inflammatory condition of unknown origin. Focal myositis can be mistaken for sarcomas, deep vein thrombosis, or infectious processes but is distinguished by its spontaneous improvement and responsiveness to non-steroidal anti-inflammatory drugs (NSAIDs). Although generally benign, focal myositis may recur. Given its generally good prognosis, it is important to differentiate it from infections or thrombosis. Less common causes of psoas muscle edema include paralysis atrophy, rhabdomyolysis, retroperitoneal fibrosis, or the presence of a foreign body (2).

The following is a rare case of psoas major delayed-onset muscle soreness (DOMS) due to bilateral stretching of the psoas muscles in a 44-year-old female patient.

CASE REPORT

A 44-year-old woman presented with hip pain persisting for two days. She reported that the pain began the day after participating in a 40-minute abdominal workout, which she had also attended two days prior. She denied any history of surgery, trauma, or numbness in her lower limbs. She weighs 70 kg and is 163 cm tall. She has worked as a bridal store manager for 25 years, where she spends all day wearing high heels and frequently climbs up and down stairs. Although she engaged in weight training, she was not accustomed to abdominal training like the ones she had recently attended.

During the physical examination, she exhibited normal mobility in her lower limbs but experienced pain when flexing and rotating her right hip, with preserved strength. Positive findings were noted on iliopsoas, Stinchfield, and Ludloff tests due to pain. The magnetic resonance imaging (MRI) was performed two days after the pain started and revealed significant edema in the psoas major muscle bilaterally, more pronounced on the right side, consistent with DOMS of the psoas major muscles (Figure 1).

The patient rested and received analgesic treatment with dipyrone and physiotherapy, resulting in resolution of pain within two weeks. She subsequently resumed her usual weight training routine.

DISCUSSION

DOMS is a condition marked by the appearance of muscle pain 1 to 2 days after performing an unfamiliar exercise. It is commonly linked to exercises that involve eccentric (lengthening) muscle contractions, as demonstrated in the report (4). Pain related to DOMS usually peaks between 24 and 72 hours after physical activity and then gradually subsides. This clinical pattern differs from muscle strains, where pain occurs immediately, and this distinction is crucial for accurate diagnosis (5).

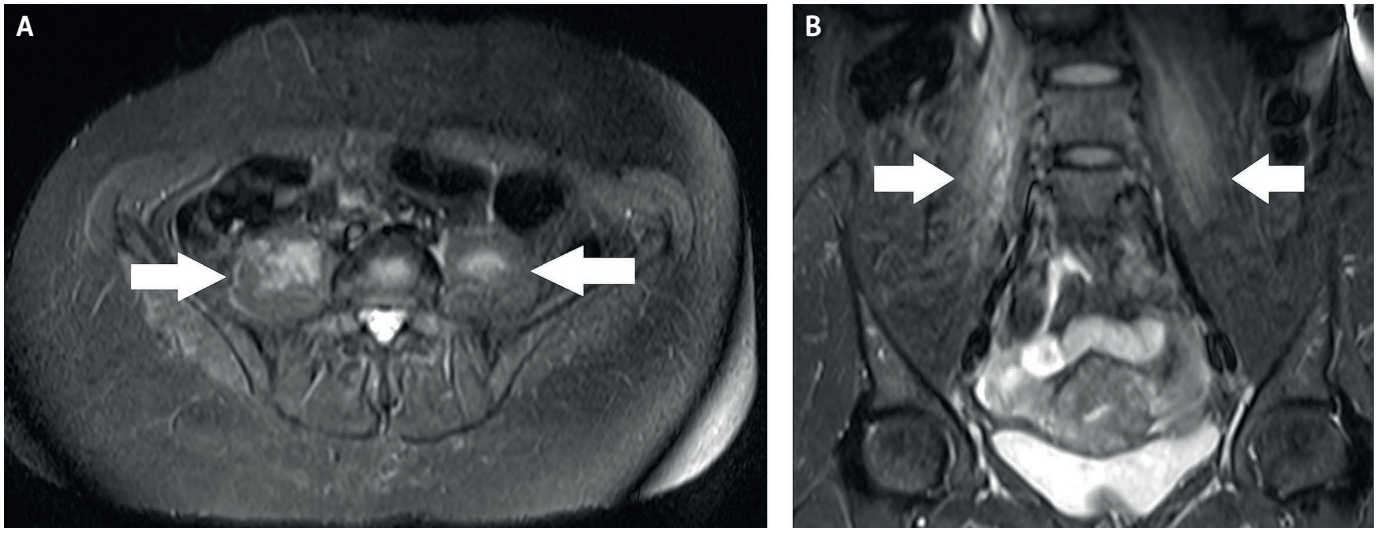

Fig. 1 T2 FAT SAT MRI in axial section (A) and coronal section (B) shows significant edema in the psoas major muscle bilaterally (white arrows), more pronounced on the right side, consistent with delayed-onset muscle soreness of the psoas major muscles.

This condition may involve temporary muscle damage visible at a microscopic level, along with elevated plasma levels of creatine kinase (CK) and, in severe instances, myoglobin in the urine. On a CT scan, a decrease in muscle attenuation and an increase in muscle volume may be observed. Ultrasound imaging can reveal edema as an increase in muscle echogenicity. On MRI, T2-weighted imaging using chemically selective fat suppression and STIR sequences, the affected muscles exhibit high signal intensity, with the amount of muscle edema on MRI correlating with the serum CK level. There is also some correlation between the intensity of pain (experienced during passive muscle extension) and the volume of muscle edema observed on MRI.(4) The greater intensity involvement of the right psoas major muscle in the patient reported is related to the process of motor development not trained for ambidexterity for motor coordination, there is, in the process of fatigue (strenuous physical activity), an overload on the dominant side, which in the case of the patient described, who was right-handed, the largest edema visible on MRI was in the right psoas major muscle.

DOMS does not involve any visible fiber disruption or tears. However, in some instances, may cause diffuse edema in the affected muscle belly, which does not show the characteristic "feathery" pattern seen in strains and lacks perifascial fluid (5). If the exercise that caused the soreness targeted a specific set of muscles, the imaging findings will be confined to those areas, as in the case reported in which several types of abdominal exercises overload the psoas major muscles. In contrast, if multiple muscle groups were involved, the pattern may be more widespread (4). Symptoms typically resolve, and muscle function is restored within 10 to 12 days, while abnormal signal intensity on fluid-sensitive MRI images can persist for up to 80 days (5).

Differential diagnosis is complex; pain caused by psoas major DOMS can be mistaken for various other diseases, including other musculoskeletal pathologies or visceral causes such as ureteral stones, salpingitis, hip arthritis, femoral bursitis, colon diverticulitis, and colon cancer (1).

Regarding treatment, the conservative approach is commonly utilized. Non-pharmacological treatments include specific activity modification and physiotherapy. Additionally, NSAISs are used for pharmacological purposes. Most patients respond well to conservative treatment and achieve full recovery (6).

CONCLUSION

While edema in the psoas major muscle is commonly associated with various pathological conditions such as infection, malignancy, and trauma, it can also occur due to more benign causes like DOMS. The case presented here highlights the importance of considering DOMS in the differential diagnosis of psoas muscle edema, particularly in individuals who engage in unfamiliar or intense physical activities. The patient's symptoms and imaging findings were consistent with DOMS, and she responded well to conservative treatment with rest and analgesics, with full recovery within two weeks.

This case underscores the need for clinicians to be aware of the distinct clinical and imaging features of DOMS to avoid unnecessary investigations and interventions. Recognizing the self-limiting nature of DOMS and differentiating it from other more serious conditions can prevent misdiagnosis and ensure appropriate management. Furthermore, this case illustrates the relevance of patient history, particularly recent physical activity, in guiding the diagnostic process, and also the importance of adequate monitoring by professionals during physical activity to guide the practitioner and avoid injuries.

Future studies could explore the mechanisms underlying DOMS in muscles like the psoas major, which are not typically emphasized in the context of this condition and investigate optimal management strategies for patients experiencing significant discomfort.

REFERENCES

1. Tufo A, Desai GJ, Cox WJ. Psoas syndrome: a frequently missed diagnosis. J Am Osteopath Assoc. 2012 Aug; 112(8): 522–8.
2. Voloshin AG, Smirnova NV. Paraspinal and Iliopsoas Edema as a Marker of an Iliofemoral Thrombosis: Case Series Report. SOJ Ortho Rehab. 2022; 2(1): 1–4.
3. Rajakulasingam R, Azzopardi C, Dutton P, et al. Spontaneous Isolated Iliopsoas Tendon Tear in Elderly-Case Report and Review of Literature. Indian J Radiol Imaging. 2021; 31(3): 719–720.
4. McMahon CJ, Wu JS, Eisenberg RL. Muscle edema. AJR Am J Roentgenol. 2010 Apr; 194(4): W284–92.
5. Guermazi A, Roemer FW, Robinson P, Tol JL, Regatte RR, Crema MD. Imaging of Muscle Injuries in Sports Medicine: Sports Imaging Series. Radiology. 2017 Mar; 282(3): 646–663. Erratum in: Radiology. 2017 Dec; 285(3): 1063.
6. Dydyk AM, Sapra A. Psoas Syndrome. 2023 Jun 21. In: StatPearls (Internet). Treasure Island (FL): StatPearls Publishing, 2024.